vehicles

MDPI

Review

A Review of Recent Trends in High-Efficiency Induction Motor Drives

Mohamed Azab

Electrical Engineering Department, Yanbu Industrial College, Yanbu 46452, Saudi Arabia; mohamed.ahmed.azab@ieee.org

Abstract: Induction motor (IM) drives are considered one of the important technologies in modern industry. Several industrial applications, such as material handling and food and beverage applications, are driven and operated by modern AC drives. Moreover, modern electric transportation systems such as EVs and e-trucks are based on AC drives. Recently, high-efficiency IM drive systems have been studied as a major opportunity to reduce energy and fuel consumption. This article addresses the recent trends and advancement in high-efficiency IM drives during a particular period (2017–2024), including the development of high-efficiency motors, the utilization of efficient wide bandgap (WBG) semiconductor devices for inverter topology, and commonly used control strategies to achieve high-performance drives. Moreover, the article addresses several manufacturers of industrial IM drives and the corresponding adopted control techniques in their products. A comparison of these control techniques, including their pros and cons, has been conducted as well.

Keywords: electric drives; AC drives; induction motor; electric vehicles; EV; efficiency; energy saving; energy efficiency; power electronics; wide bandgap semiconductors; electric motors; field-oriented control; direct torque control; model predictive control; industrial automation; regenerative braking; SDG; sustainable development goals; united nations

check for updates

Academic Editors: Adolfo Dannier and Mohammed Chadli

Received: 16 December 2024
Revised: 21 January 2025
Accepted: 5 February 2025
Published: 11 February 2025

Citation: Azab, M. A Review of Recent Trends in High-Efficiency Induction Motor Drives. *Vehicles* **2025**, 7, 15. https://doi.org/10.3390/vehicles7010015

Copyright: © 2025 by the author. Licensee MDPI, Basel, Switzerland. This article is an open access article distributed under the terms and conditions of the Creative Commons Attribution (CC BY) license (https://creativecommons.org/licenses/by/4.0/).

1. Introduction

1.1. Market Size of Electrical Drives

The demand for electric drives (EDs) across various industrial sectors and applications is growing. Owing to the latest published reports [1], the global market size for EDs is estimated at USD 25.51 billion in 2024, and is expected to reach USD 32.70 billion by 2029, growing at a compound annual growth rate (CAGR) of 5.10% during the period of 2024 to 2029 [1].

Meanwhile, the global market size of AC drives accounts for an estimated value of USD 17.9 billion in 2022, and is projected to reach USD 25 billion by 2028 at a compound annual growth of 5.7% [2]. Figures 1 and 2 indicate the global market size of electrical drives and AC drives, respectively.

1.2. Electric Drives and UN-SDGs

During the last decade, the demand for efficient electric drives (ED) has increased significantly to reduce energy consumption and enhance environmental conservation in accordance with the sustainable development goals (SDGs) of United Nations (UN), and directly linked to SDGs 7, 9, 12, and 13, which are related to energy efficiency, sustainable and clean industries, and climate action to reduce greenhouse gas emissions, respectively.

Owing to the latest published reports [3,4], significant acceleration is still needed to meet the target (see Appendix A to recognize the SDGs goals).

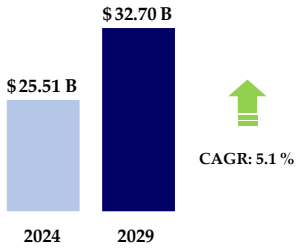


Figure 1. Estimated global market size of electrical drives.

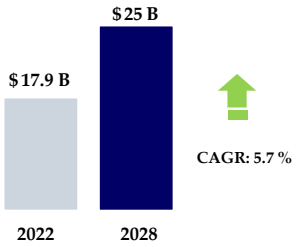


Figure 2. Estimated global market size of AC drives.

Therefore, high-efficiency AC drives play a considerable role in tackling some of the world's greatest challenges and achieving a sustainable and equitable future. The high-efficiency drives are characterized by minimal energy consumption and significant energy savings, resulting in less fuel consumption and a significant reduction in carbon emissions. These positive consequences support the transition to more sustainable energy use, aligning with the UN-SDGs. The wide spread of these high-efficiency drives promotes the development of more eco-friendly technologies, enhancing energy efficiency across various sectors. As mentioned before, the utilization of high-efficiency electric drives helps mitigate greenhouse gas emissions, contributing to global efforts to limit global warming [5,6].

1.3. Main Contribution

This paper presents a literature summary of the state-of-the art advancements in high-efficiency induction motor drives during a particular period (2017–2024), including high-efficiency electric motors, low power losses power semiconductor devices, and advanced control techniques that essentially contribute to improving the overall AC drive efficiency in accordance with energy efficiency guidelines and standards. In addition, the paper provides a literature summary of recent regenerative braking methods and energy saving algorithms incorporated with the induction motor control system. Moreover, the article provides a list of well-known industrial IM drives produced by several manufacturers, including their adopted control techniques. A comparison has been made between these control techniques, highlighting their pros and cons.

1.4. Elements of a Typical EDS

The generalized block diagram of a typical electric drive system (EDS) is illustrated in Figure 3. A typical EDS is composed of the following elements: mechanical load, electric motor, power source, power electronic converter (power conditioner), control unit, and measuring devices (sensors and transducers).

Simply, the main objective of an EDS is to drive a mechanical load at any desired speed/position and torque requirements using an electric motor that is fed from a power

source through a proper power electronic converter. The high-performance EDS operates in closed-loop mode, such that the motor can run at the desired speed apart from the load variation or any transient variations in the input voltage that feeds the EDS [7].

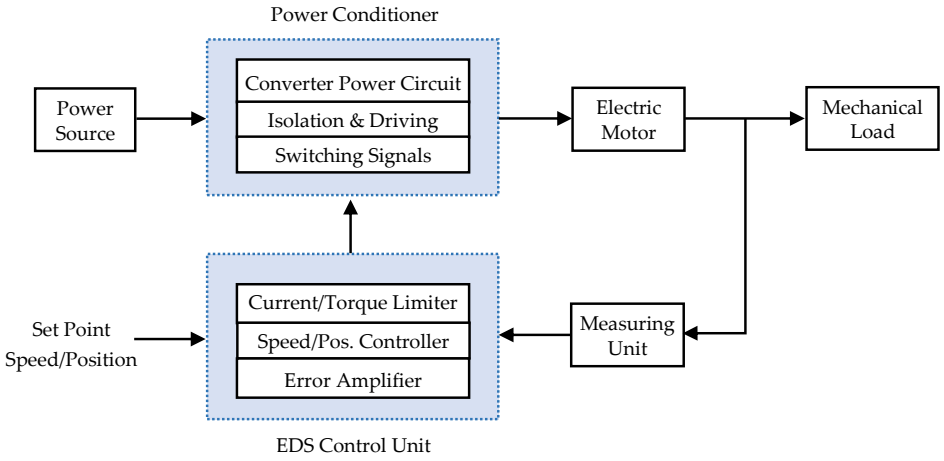


Figure 3. Block diagram of a typical electric drive system.

Practically, the block diagram of the high-efficiency EDS is like the conventional EDS. The major differences between both systems are considered in the following points:

1. Efficiency classes of the electric motor, where high efficiency and premium efficiency classes are employed;
2. Types of the power semiconductor devices that form the power electronic converter, where a high-efficiency converter that offers minimum power losses is utilized;
3. Control techniques, which can involve energy saving algorithms or guarantee operation at optimum flux level for a wide range of motor speeds.

1.5. Factors Affecting Efficiency of IM Drives

The key factors that affect directly the overall efficiency of the IM drives are related mainly to motor design, operating conditions, environmental conditions, periodic checkup rate, and maintenance status. The breakdown of these factors is summarized in Table 1.

Table 1. Key factors affecting overall efficiency of IM drives.

Key Factors		Related Items
Motor	Motor Design	Slot design, air gap length, core material, winding design, stator and rotor dimensions and materials, ventilation and cooling system
	Operating Conditions	Type of loading, percentage of loading related to the full load (FL), operating speed, harmonics due to inverter & total harmonic distortion (THD) of load current
	Environmental Conditions	Ambient temperature, dust and humidity, mechanical vibrations
	Checkup and Maintenance	Status of bearing and lubrication, quality of winding insulation
PE Converter	Power Semiconductor Type	On-resistance, switching characteristics, driving requirements
	Converter Cooling	Heatsink design, cooling type (forced air, forced water)
	Operating Conditions	Switching frequency, load current, supply voltage
	Hardware Topology	Conventional two-level inverter, multilevel, number of power devices of emerging topologies
	Switching Strategy	Hard switching, soft switching, PWM technique
	Environmental Conditions	EMI, ambient temperature, dust and humidity

1.6. Power Losses in IM Drives

The previously mentioned factors of Table 1 can be optimized to achieve a high-efficiency AC drive. Practically, the corresponding items of Table 1 contribute to various power losses across the elements of the AC drive, which altogether affects the overall efficiency of the IM drive. Accordingly, the main types of power losses in IM drives can be summarized in the following points:

1. Copper losses across the motor windings;
2. Magnetic (iron) losses of the magnetic circuit;
3. Losses in rotor windings (in wound rotor) or cage losses (in case of squirrel cage);
4. Iron losses or core losses including hysteresis and eddy currents losses;
5. Mechanical and bearing losses due to friction;
6. Stray losses due to leakage flux, magnetic imperfections;
7. Switching power losses of the inverter;
8. Conduction power losses of the inverter;
9. Cooling system losses due to fans (forced air), liquid cooling and heat sink thermal resistance;
10. Inverter driving circuits power losses;
11. Snubber circuits and passive filters power losses.

Thus, minimization of all these types of losses by optimum design of the AC motors, utilizing efficient power semiconductor devices, optimizing the drive cooling, and adopting proper control strategy permits considerable energy saving and enhances the overall efficiency of the electric drive system.

1.7. Advancement Directions in IM Drives

The advancement in IM drives has many directions. The major trends include:

1. Replacement of conventional IM motors by high-efficiency and premium-grade counterparts [8,9];
2. Utilization of wide bandgap (WBG) semiconductors [10,11];
3. Implementation of modern control techniques such as: direct torque control (DTC) proposed by authors of [12], model predictive control (MPC) [13], and incorporation of regenerative braking and energy saving algorithms to reduce energy consumption [14,15];
4. Utilization of efficient high-speed digital signal processors (DSP) as core processors [16], and involvement of hardware in the loop (HIL) data acquisition cards for rapid prototyping and testing purposes [17,18].

Discussions of such directions are presented in Sections 2–5 as follows: Section 2 provides an overview of the state-of-the-art advancement in high-efficiency induction motors that are commonly used in IM drives. In fact, induction motors are only considered in this article to limit the study and the article length. Section 3 addresses the major trend in high-efficiency power electronic converters based on (WBG) semiconductor devices. Section 4 presents an overview of the advanced control techniques utilized to achieve high-performance IM drives. Section 5 highlights key manufacturers of induction motor drives and the employed control techniques. In addition, some applications of IM drives are addressed in Section 6.

2. High-Efficiency Induction Motors

In general, motor design plays an important role in achieving higher efficiency [19,20]. Several types of AC motors are commonly used and employed in modern electric drive systems. Thus, obtaining high-efficiency AC drives depends on utilization of high-efficiency

AC motors. Induction motors (IMs) are considered the most important rotating machines that remain widely used in the modern industry due to their simplicity and reliability.

2.1. Main Features of High-Efficiency IMs

Compared with the standard types of 3-Φ induction motors, whose cross section of their stator is illustrated in Figure 4, and the rotor of squirrel case types, depicted in Figure 5, the high-efficiency counterparts have the following features:

1. Longer core (motor) length;
2. Thinner core lamination;
3. High grade core material such as grain-oriented silicon steel;
4. Wider stator slots with optimized shapes (based on finite element design and analysis);
5. Thicker stator windings (larger winding cross section area);
6. High temperature electrical insulation class;
7. Larger rotor diameter;
8. Lower resistance rotor bars such as die cast copper rotor;
9. Narrower air gap between the stator and rotor;
10. Larger fan size with optimized aerodynamic;
11. Larger cooling fins and increase cooling surface area;
12. Small bearing size with lower friction losses;
13. Anti-corrosion coating for the motor body.

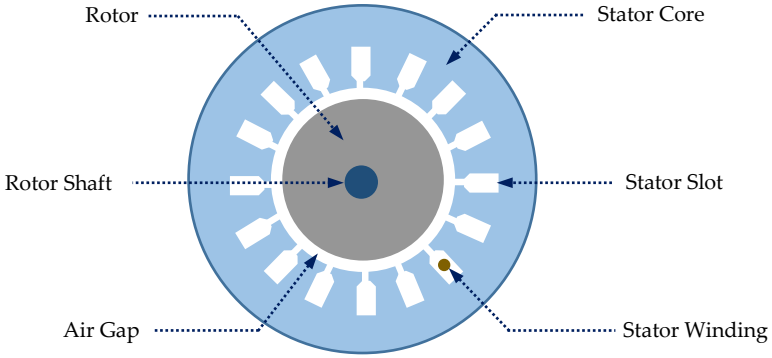


Figure 4. Cross section of stator of a 3-Φ induction motor.

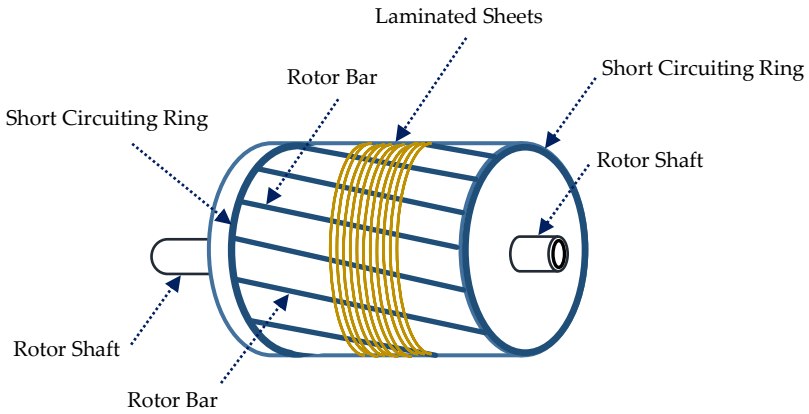


Figure 5. Rotor of a squirrel cage of a 3-Φ induction motor.

Due to the importance of the topic, several research efforts have been exerted during this decade to improve the performance of IMs in terms of minimizing power losses, improving the starting characteristics, or adopting new approaches for design optimization, such as development of bearingless motors for high-speed applications. Recent improve-

ments in rotor designs and stator winding configurations have led to significant efficiency gains [21–23].

2.2. Research Contributions Related to High-Efficiency IMs

A summary of the major research contributions in high-efficiency IMs during the period of 2017–2024 are presented in Tables 2–6. The survey of core contributions includes the following main areas:

1. Design and manufacturing of high- and premium-efficiency induction motors (Table 2);
2. Optimization techniques and algorithms for high efficiency motor design (Table 3);
3. Efforts in bearingless IMs (Table 4);
4. Modeling, loss analysis, and computational tools (Table 5);
5. Thermal analysis and cooling systems (Table 6).

Table 2. Research contributions related to design and manufacturing of high-efficiency IMs.

Main Area	Ref.	Core Contribution
Design and Manufacturing of High-Efficiency Motors	[9]	Design of an energy-efficient IM by combining field-circuit and analytical methods; the authors optimized the motor's core materials and structure to minimize power losses.
	[21,22]	Analyzing and validating different rotor slot geometries to enhance the motor efficiency and starting performance.
	[23]	Motor design and fabrication using amorphous alloy instead of silicon steel, reducing the core and copper losses.
	[24]	Design of a high-performance IM using flat wires and a copper rotor tailored for EVs, demonstrating the feasibility of a rare-earth-free solution that achieves a high-efficiency and thermally stable motor.
	[25]	Designing a six-pole, double-stator–double-rotor axial flux induction motor designed for electric vehicles. The innovative design reduces back iron thickness, leading to a more compact and efficient motor.
	[26]	Developing a low-cost IM with a totally enclosed fan-cooled aluminum cage rotor suitable for EVs.
	[27]	Modifying stator and rotor designs to minimize losses, using low-loss electrical steel and high-conductivity copper to comply with the premium-efficiency class.
	[28]	Analyzing the trade-offs between cost, thermal performance, and efficiency, recommending an optimal Al-Cu mix to achieve IE4 efficiency standards.
	[29]	Investigating the effects of end-ring geometric parameters (thickness, height, and extension) on the starting and rated performance characteristics of IMs.
	[30]	Presenting a methodology for designing energy-efficient induction motors using ANSYS software. Motor parameters are optimized with the aid of FEM.
	[31]	Designing of electric motors and power drive systems in compliance with contemporary efficiency standards. Addresses the importance of integrating efficiency considerations in the early design stage.
	[32]	Analyzing the impact of substituting aluminum with copper in squirrel cage induction motors. Evaluation of electromagnetic and thermal performance, revealing that copper cages enhance efficiency but may affect starting torque. Design guidelines to optimize motor efficiency are also presented.
	[33]	Presenting strategies for induction motor manufacturers to achieve higher efficiency classes in terms of material selection, manufacturing processes and design parameters.

Table 2. *Cont.*

Main Area	Ref.	Core Contribution
Design and Manufacturing of High-Efficiency Motors	[34]	Enhancing the efficiency of three-phase squirrel cage induction motor by modifying its cooling system. Suggesting the utilization of aluminum for the stator housing, rotor bars, and end rings to raise the efficiency.
	[35]	Optimizing rotor and stator slot designs of induction motor that is employed for photovoltaic (PV) powered water pumping systems
	[36]	Presenting a design of high-efficiency IM based on modifying the rotor lamination, stack length, and winding configuration while retaining the existing stator lamination.
	[37]	Introducing a stator winding scheme for IMs aimed at reducing magnetomotive force (MMF) distortion. Based on a three-layer winding with varying conductor counts per slot, which has minimized harmonic components in the MMF waveform.
	[38]	Designing a cryogenic induction motor submerged in liquefied natural gas (LNG) for operating LNG spray pumps, operating at −163 °C; the motor's torque characteristics differ significantly from room temperature conditions. Main design specifications for optimal performance in cryogenic environments have been addressed.
	[39]	Providing a comprehensive overview of the design and control methodologies for improving the energy efficiency of electric machines, including IMs, used in EVs. Also evaluates the impacts of stator and rotor designs, winding configurations, and novel materials on energy efficiency.
	[40]	Investigating the utilization of magnetic slot wedges in IMs with semi-closed slots to enhance efficiency. Various wedge permeabilities and geometries have been studied, demonstrating reductions in copper and core losses.
	[41]	Presenting a methodology to enhance the efficiency of IMs operating at low frequencies by integrating design modifications with control strategies. Motor parameters are optimized by achieving significant energy savings.

Table 3. Research contributions related to optimization techniques for high-efficiency IMs.

Main Area	Ref.	Core Contribution
Optimization Techniques and Algorithms for High-Efficiency Motor Design	[23]	Design optimization via evolutionary algorithms to optimize the stator and rotor slot shapes, achieving a balance between reduced losses and maintained performance
	[25]	Employment of a Monte-Carlo random search algorithm to optimize the motor parameters.
	[26]	Presenting an optimal design and experimental testing of a low-cost, totally enclosed fan-cooled induction machine for city battery electric vehicles. Combines thermal calculations, and finite element analysis (FEA) to enhance the design process by minimizing prototype iterations and ensuring multi-disciplinary performance.
	[28]	Optimizing the motor efficiency by optimal combination of Al-Cu that can meet IE4 standards.
	[29]	Optimizing end-ring thickness to improve starting performance without major changes to existing designs, with a slight trade-off in efficiency, moving from IE4 to IE3 class.
	[42]	Optimizing the motor design via evolutionary algorithms to optimize the stator and rotor slot shapes, achieving a balance between reduced losses and maintained performance. Optimizing motor parameters to enhance efficiency for ceiling fan motors using Taguchi's Orthogonal Arrays method.

Table 3. *Cont.*

Main Area	Ref.	Core Contribution
Optimization Techniques and Algorithms for High-Efficiency Motor Design	[43]	Developing a design procedure focused on field-weakening and extended-speed capabilities. The key parameters are EMF and inductance-current product.
	[44]	Development of a hybrid optimization algorithm, combining differential evolution with a non-dominating sorting algorithm, minimizes both the air gap MMF spatial harmonic distortion and the winding resistance, using a hybrid algorithm. The approach yields a winding configuration that reduces copper usage and enhances motor efficiency.
	[45]	Utilization of a machine learning-based approach for diagnosing faults and efficiency optimization in induction motors (IM) for electric vehicle EVs. This approach enables early fault detection, enhances motor reliability, and reduces maintenance costs.
	[46]	Utilization of genetic algorithms to optimize eight key parameters of linear induction motors (LIMs), improving efficiency at rated operating conditions.
	[47]	Introducing a sequential Taguchi method to optimize IM designs for electric vehicles, focusing on various stator slot and rotor bar combinations.
	[48]	Introducing a fractional-order finite element model to analyze the harmonic response of vehicle asynchronous motor rotors. An accelerated response surface optimization method to enhance rotor stiffness and reduce mass is proposed.
	[49]	Assessing various strategies to enhance induction motor efficiency. Impact of design modifications and material selection on the motor performance have been evaluated to achieve higher efficiency of IMs.
	[50]	Introducing a multilayer AC winding configuration for IMs to produce a high-quality magnetomotive force (MMF) with reduced space harmonics for a premium efficiency class machine.
	[51]	Studying the effect of stator slot geometry on the copper losses in high-speed electric machines. Identifying the optimum designs that mitigate skin and proximity effects.
	[52]	Presenting an optimization methodology for the stator and rotor slot design of IMs for EV applications. Utilizing FEM analysis, various slot geometries are investigated to minimize losses and enhance efficiency.
	[53]	Presenting a genetic algorithm-based approach to optimize the design of squirrel cage induction motors, to enhance motor efficiency and minimize costs. Material, mechanical, and performance constraints are incorporated to offer a systematic method to achieve energy-efficient motor designs.
	[54]	Introducing a multi-objective optimization approach for designing high-efficiency induction motors using parameter learning. The objectives terms are efficiency, torque ripple, and power factor.
	[55]	Presenting harmony search algorithm for optimizing the design of three-phase squirrel-cage IMs. The method explores nonlinear design items to enhance motor efficiency.
	[56]	Introducing a multi-objective optimization technique for IM design, utilizing Hill Climbing-based Local Search Optimization (HCLSO). The method iteratively investigates problems such as rotor current, power factor, and efficiency to enhance the motor performance.

Table 4. Research contributions related to development of bearingless IMs.

Main Area	Ref.	Core Contribution
Bearingless IMs	[57]	Proposing a speed sensorless control strategy for bearingless induction motors (BIM) using a modified robust Kalman filter. This method enhances the accuracy of speed estimation and robustness against disturbances.
	[58]	Introducing a direct torque control strategy for bearingless induction motors, employing super-twisting sliding mode control to enhance performance. The employed approach reduces torque and flux ripples and improves robustness against parameter variations.
	[59]	Introducing an enhanced repetitive control strategy to mitigate periodic synchronous rotor vibrations in bearingless induction motors, improving rotor suspension accuracy.
	[60]	Presenting a backstepping control strategy for bearingless induction motors, enhanced by a linear extended state observer (LESO). The utilized approach compensates for the system disturbances, enhancing rotor suspension performance and disturbance rejection.
	[61]	Proposing a fuzzy-enhanced linear active disturbance rejection control (Fuzzy-ELADRC) method for bearingless induction motors. The method combines dynamically adjust control parameters, balancing dynamic performance and robustness. The investigated method improves rotor suspension stability.
	[62]	Providing a multi-objective optimization framework based on evolutionary algorithms to optimize the design of high-speed bearingless induction motors (IMs), aiming to enhance efficiency and power density.
	[63]	Offering systematic design and modeling of a high-performance bearingless induction motor (IM) suitable for medium to high power applications.
	[64]	Developing a rotor radial position control method for bearingless IMs, aimed at enhancing machine stability, reducing mechanical vibration, and controlling rotor eccentricity.
	[65]	Providing a comprehensive review of bearingless motor technology. The paper reviews the motor designs, different topologies, and their performance. It discusses the major limitations in achieving the efficiency and power density for large-scale applications.
	[66]	Proposing a winding design for bearingless motors, enabling a single winding to generate both torque and radial suspension forces. The main feature is separating the terminals for torque and suspension, where the suspension terminals do not contribute a motional electromotive force when the rotor is centered.
	[67]	Investigating a pole-specific rotor design for bearingless induction machines, characterized by a common end-ring to reduce axial length, improving efficiency by preventing suspension field-induced currents.
	[68]	Proposing a three-speed wound bearingless induction motor with a novel winding configuration that enables operation at multiple synchronous speeds. That design enhances the efficiency and stability of the motor.
	[69]	Introducing a speed sensorless control strategy for bearingless induction motors based on an adaptive flux observer. This method improves the rotor suspension performance under various operating conditions.
	[70]	Proposing a driving scheme for three-phase bearingless induction machines with split windings, reducing the required inverter legs from six to four, which decreases the number of drivers, sensors, and current controllers, reducing the overall cost.
	[71]	Providing a comprehensive review of bearingless induction motors, addressing principles of operation, different schemes, and key technologies and challenges.
	[72]	Investigating a model predictive control strategy for direct levitation force control in bearingless induction motors. This approach enhances rotor suspension stability and dynamic response under various operating conditions.

Table 4. *Cont.*

Main Area	Ref.	Core Contribution
Bearingless IMs	[73]	Addressing a design framework for bearingless induction motors tailored for industrial compressors. It has a pole-specific rotor winding and a combined stator winding.
	[74]	Suggesting a fuzzy logic controller for the radial position control of a bearingless induction motor, resulting in improved rotor stability and performance.
	[75]	Proposing a driving method for a two-degrees-of-freedom controlled bearingless motor, utilizing a single three-phase inverter. The staggered-tooth stator core design facilitates starting torque production. The method guarantees effective control over both rotational and radial movements.
	[76]	Studying a novel direct torque control method for bearingless induction motors using sliding mode control, incorporating a closed-loop radial suspension force control method based on inverse system theory. A stable suspension operation with reduced torque that enhanced both dynamic response and suspension performance was observed.

Table 5. Research contributions related to modeling, analysis, and computational tools for high-efficiency IMs.

Main Area	Ref.	Core Contribution
Modeling, Loss Analysis and Computational Tools	[24]	Designing a 200 kW induction motor for electric vehicle traction systems, utilizing flat wire windings and a copper rotor. The design improves the slot fill factor. The study provides a comprehensive analysis of material selection and design considerations.
	[25]	Development and validation of a detailed equivalent circuit model for the double-stator–double-rotor configuration using ANSYS Maxwell, providing efficient motor design.
	[28]	Investigating and analyzing the performance of IE4-class IMs with rotor conductors composed of varying aluminum–copper (Al-Cu) ratios. This approach aims to enhance motor efficiency while managing manufacturing costs.
	[44]	Developing a generalized multilayer winding model for symmetrical AC machines, incorporating integer-slot, fractional-slot, and fractional-slot concentrated windings.
	[45]	Development of ML models and simulation of various faults, including Short Circuit (SC), High Resistance Connection (HRC), and Open-Phase Circuit (OPC), and generation of performance data for both healthy and faulty motor conditions under variable load conditions, achieving high accuracy (up to 100%) in identifying motor conditions.
	[46]	Development of an integrated loss model for optimal efficiency control incorporating both motor and inverter losses for enhanced efficiency.
	[62]	Proposing and developing computationally efficient finite element analysis (FEA) methods that allow rapid design performance evaluations, and optimizing the bearingless IM design without excessive computation time.
	[63]	Introducing various finite element analysis (FEA) methods, including a modified transient FEA model, which allow for rapid and accurate performance evaluations.
	[64]	Finite element analysis (FEA) which validates the control approach, demonstrating reliable rotor positioning and reduced eccentricity.
	[77]	Presents a computationally efficient model for analyzing AC winding losses in the stator of traction motors used in high-speed railway units. The model reduces computational demands compared to conventional methods. The model is validated through experimental data and compared with other existing models, demonstrating high accuracy with significantly reduced computational cost. It can help in optimizing motor design to reduce winding losses.

Table 5. *Cont.*

Main Area	Ref.	Core Contribution
Modeling, Loss Analysis and Computational Tools	[78]	Carrying out harmonic and unbalance sensitivity analysis on efficiency motors. It investigates the balance between achieving higher energy efficiency motor and the potential degradation in power quality under nonideal electrical supply conditions.
	[79]	Providing a framework for evaluating the practical and economic impacts of upgrading to high-efficiency electric motors. The study examines the criteria used to assess the feasibility of replacing standard efficiency motors with high-efficiency motors.
	[80]	Proposing a dynamic model for a bearingless induction motor, accounting for rotor eccentricity and load variations. It introduces a modified inductance model and a dynamic air gap function to more accurately depict system behavior, improving the system stability and accuracy of the control system.
	[81]	Introducing a multi-physics model to predict motor performance of axial flux induction motors for EVs. Employs a genetic algorithm-based optimization strategy to enhance efficiency, torque density, and power-to-weight ratio, resulting in better performance and reduced energy consumption in the overall EV.
	[82]	Proposing a machine learning-based method for diagnosing faults in IMs using stator current and vibration signals. This approach enhances diagnostic accuracy.
	[83]	Holding comparison between several IM models that account for iron loss in EVs. Models' accuracies at different operating conditions have been investigated.
	[84]	Proposing an analytical core loss model for three-phase IMs in an arbitrary reference frame. Accurately predicts core losses under various operating conditions, including transient operation.

Table 6. Research contributions related to thermal analysis and cooling systems for high-efficiency IMs.

Main Area	Ref.	Core Contribution
Thermal Analysis and Cooling Systems	[24]	The study explores two cooling solutions: water jacket with spiral groove and oil spray methods, to manage heat dissipation at high speeds, crucial for maintaining efficiency and component longevity.
	[85,86]	Providing a comprehensive review of thermal management techniques and cooling strategies for high-efficiency IMs. Addresses major thermal challenges, analysis techniques, and evaluate different cooling strategies.
	[87]	Development of a novel oil-cooling design for IMs utilized in EV applications. Addresses the thermal constraints. Demonstrates the importance of thermal management through oil cooling in enhancing motor reliability and lifespan.
	[88]	Addressing the various types of losses in electric machines. Explores various cooling techniques. Emphasizes the importance of temperature distribution analysis and the role of heat management in enhancing machine reliability and operational lifespan.
	[89]	Presenting a thermal analysis method for IMs using a Lumped Parameter Thermal Network model. Accurately predicts motor temperature distribution under varying load conditions, enhancing thermal management and preventing overheating.
	[90]	Providing a thermal analysis of a water-cooled, totally enclosed, non-ventilated IM. Develops a detailed thermal model to evaluate temperature distribution and cooling efficiency. The study highlights the effectiveness of water cooling of IM and enhancing its reliability.

Table 6. *Cont.*

Main Area	Ref.	Core Contribution
Thermal Analysis and Cooling Systems	[91]	Proposing a hybrid thermal management system for IMs, combining air-cooling with an integrated water-cooling mechanism that optimizes motor cooling and improves thermal efficiency. The dual-cooling approach enhances motor reliability, and lifespan.
	[92]	Investigating the impact of cryogenic cooling on the performance of induction motors through experimental assessment. The study highlights cryogenic cooling as a promising approach for high-performance applications.
	[93]	Exploring the heat transfer performance of cooling systems using nanofluids for electric motors. Analyzes the cooling efficiency of nanofluid-based systems. The findings reveal enhanced cooling performance compared to conventional fluids, offering a novel approach to improve motor thermal management.
	[94]	Conducting a thermal analysis of a three-phase IM using Motor-CAD, Flux2D, and MATLAB Ver 13. Integrates electromagnetic and thermal simulations to predict temperature distribution and assess cooling performance. This multi-tool approach enhances motor design accuracy and improves thermal management.
	[95]	Analyzing the thermal behavior of three-phase IM under voltage unbalance and inter-turn short-circuit faults. Investigates the fault-induced heating effects and their impact on the motor performance.
	[96]	Providing a finite element design and thermal analysis of IMs. Develops a thermal model to predict temperature distribution, ensuring optimal motor cooling and enhanced performance. The study provides a design framework for thermally robust IM motors.
	[97]	Proposing a thermal management system for electric motors using L-shaped flat heat pipes. Demonstrates the heat pipes' effectiveness in dissipating heat, reducing motor temperature and enhancing thermal stability.
	[98]	Providing analysis of end-winding thermal effects in an enclosed fan-cooled induction motor with a die-cast copper rotor. Models heat generation and dissipation in the end-windings, highlighting their impact on motor temperature and performance.
	[99]	Developing a thermal model for IMs with optimized liquid cooling tailored for different electric vehicles (EVs). Assesses cooling performance, reduces motor overheating, and enhances thermal stability under dynamic conditions.
	[100]	Presenting an optimal design methodology for the cooling fan of IMs using experimental validation. Enhances airflow and reduces motor temperature. Provides a systematic approach for fan design.
	[101]	Proposing an optimization method for the design of traction motor cooling system. The integrated thermal modeling and design algorithms enhance motor cooling efficiency.
	[102]	Establishing design criteria and framework for water-cooled systems in IMs. Addresses key parameters such as flow rate and cooling channel geometry. The study optimizes heat dissipation and reduces motor temperature and enhances system reliability.

Moreover, the efficiency ranges of typical premium efficiency IMs, fabricated by key manufacturers for different power ratings, are presented in Table 7.

Table 7. Technical data and efficiency ranges of typical high-efficiency induction motors.

Series	Rating Range	Manufacturer				
		ABB [103]	**AEG [104]**	**WEG [105]**	**LEADGO [106]**	**TOSHIBA [107]**
Premium Efficiency	0.75–22 kW	82.5–93.6%	82.5–93%	85.5–93%	82.5–90%	82.2–94.1%
	30–110 kW	94.1–95.8%	93.6–95.4%	93.6–95.4%	93.6–95.4%	94.1–95.3%

Table 7 summarizes the corresponding efficiency ranges of typical premium efficiency IMs fabricated by different manufacturers [103–107]. For a power rating between 0.75 kW and 22 kW, the corresponding efficiencies are between 82.5% and 93.6%, while for a higher power rating between 30 kW and 110 kW, the corresponding efficiencies are between 93.6% and 95.8%.

3. Wide Bandgap (WBG) Power Semiconductor Devices

The transition from silicon (Si)-based semiconductor devices to wide bandgap (WBG) semiconductors devices is considered one of the most significant advancements in improving the overall efficiency of the power electronic converters [108,109]. Basically, the bandgap is defined as the minimum energy required to excite electrons, transferring the electrons from the valence band to the conduction band.

3.1. Characteristics of WBG Semiconductors

Compared to the conventional Si-based semiconductors, the WBG semiconductors have a larger (wider) bandgap, approximately three times wider. As illustrated in Figure 6, WBG semiconductors (SiC and GaN) have a bandgap between 3.3 eV and 3.4 eV, allowing the WBG power devices to withstand higher voltages (high breakdown voltage) due to the direct correlation between the bandgap and the critical breakdown (electric) field of a semiconductor. As a typical value, the critical electric field of WBGs semiconductors is approximately ten times greater than that of Si semiconductors (0.3 MV/cm in Si, 3.5 MV/cm in SiC, and 3.3 MV/cm in GaN). Consequently, the breakdown voltage in WBG devices is higher than that of conventional Si devices.

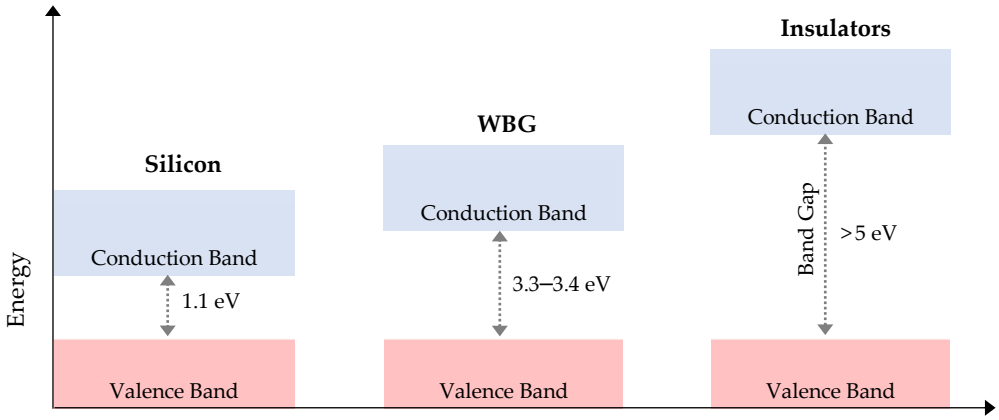


Figure 6. Simplified energy diagram and bandgap energy of Si, WBG, and insulators.

However, there are some main differences in several characteristics of SiC and GaN that make each type more convenient and adequate for certain applications over the other; e.g., GaN has higher electron mobility compared with SiC (GaN:1500 cm^2/Vs, Sic: 900 cm^2/Vs). This means GaN devices are characterized by high switching frequencies, which makes them more suitable for high frequency applications.

Meanwhile, the greater thermal conductivity of SiC devices (5 W/cmK) compared with that of than GaN (1.3 W/cmK) makes SiC devices transfer heat more efficiently, enabling operation at higher temperatures and allowing higher power densities as well. Thus, the distinct characteristics of each type of WBG devices make GaN suitable for low-power and high-frequency applications, while they make SiC suitable for high-power and high-voltage applications [110,111]. Compared to traditional Si-based devices, WBG devices offer superior performance in terms of higher switching frequencies, lower power losses, and high temperature capability. These advantages have permitted their utilization in

various applications such as high-performance industrial drives [112,113], electric vehicles (EVs) [114,115], aircraft propulsion [116], and renewable energy applications [117,118]. The utilization of SiC power devices in motor drives can reduce the overall cost of the drive by decreasing the size of passive components [119,120].

3.2. Main Challenges and Design Issues

Compared with the Si power devices, the WBG power devices face some obstacles and challenges that limit their industrial utilization and delay achieving commercial acceptance and full satisfaction. Some of these challenges are:

1. Higher fabrication and manufacturing cost;
2. Complex fabrication processes to have the final product with good quality;
3. Reliability issue for GaN devices at high temperature;
4. Cooling system design and analysis;
5. Requirement of proper packaging to alleviate electromagnetic interference (EMI).

Fortunately, the fabrication costs of SiC devices are expected to decline as companies move toward the technology of six-inch wafers [120].

Several design issues are taken into consideration during design and testing of WBG-based power electronic converters to achieve successful and reliable operation [121–125]. The main important design issues that are related directly to the successful and reliable operation of the WBG-based power electronic converter are:

1. Gate driving signals (voltage levels), which are different from the well-known and commonly used values of Si devices;
2. The effect of parasitic inductance at operation of high switching frequencies, which requires compact and optimized PCB designs;
3. EMI and electromagnetic compatibility (EMC) concerns due to high dv/dt and di/dt.

3.3. Research Contributions Related to WBG-Based Converters and AC Drives

A summary of the major research contributions is presented in Tables 8–11. The survey of core contributions includes the following main areas:

1. Performance analysis of WBG devices, inverters, and IM drives (Table 8);
2. System design and performance improvement (Table 9);
3. Thermal management and cooling systems (Table 10);
4. Key challenges and solutions (Table 11).

Table 8. Research contributions related to performance analysis of WBG devices and systems.

Main Area	Ref.	Core Contribution
Performance Analysis	[11]	Investigating the effects of high switching speeds and frequencies in wide bandgap (WBG) motor drives on electric machines. Identifies increased motor overvoltage at terminals and stator neutral, leading to higher insulation stress and bearing currents.
	[109]	Proposing a hybrid DC–AC topology combining a Si-IGBT master unit with selective harmonic elimination PWM and a partial-power SiC-MOSFET slave unit. This configuration enhances efficiency, reduces switching loss, and improves power density.
	[110]	Providing comparative analysis of two-level and three-level SiC-based AC drive topologies for efficiency, voltage quality, and common-mode currents. Experimentally evaluates the impact of filters on mitigating high-frequency effects and meeting NEMA standards.
	[111]	Discussing issues such as EMI, high dv/dt, and insulation stress in case of WBG-based AC drives. Also addresses converter design trade-offs of WBG-based AC drives.

Table 8. *Cont.*

Main Area	Ref.	Core Contribution
Performance Analysis	[114]	Quantitative evaluation of energy savings and loss characteristics when replacing Si-IGBTs with SiC MOSFETs in railway traction inverters.
	[115]	Introducing a figure-of-merit (FOM) for comparing 600/650 V SiC and GaN semiconductors employed for EV drives. The paper reveals SiC's suitability for high-temperature, low-frequency applications and GaN's efficiency in high-frequency applications.
	[117]	Reviewing the state-of-the-art SiC power devices, including SiC MOSFETs and SiC SBDs, emphasizing their superior characteristics for power electronics applications.
	[118]	The paper introduces a novel integration of SiC devices with high-frequency transformers for high-power renewable energy applications. It designs and validates various DC–DC converter topologies with integrated SiC technology, achieving high efficiency (>98%), reduced size, and improved thermal management.
	[119]	Introducing a variable switching frequency PWM strategy to achieve zero-voltage switching in AC motor drives powered by two parallel SiC inverters. The scheme improves reliability and energy efficiency of AC motor drives.
	[122]	Analyzing the voltage distribution in stator windings of WBG-based inverter-fed motors, highlighting the anti-resonance phenomenon as a critical cause of peak voltage stress near the neutral point.
	[125]	Providing a comprehensive review of hybrid Si/SiC switches, highlighting their potential to combine the advantages of silicon IGBTs and silicon carbide MOSFETs for high-efficiency, high-power-density energy conversion.
	[126]	Addressing a historical overview of silicon carbide (SiC) power devices. Discusses the commercialization of SiC devices and their adoption across various applications, and offers insights into future developments in the field.
	[127]	Presenting an analytical model to predict low-frequency radiated electromagnetic interference (EMI) in three-phase motor drive systems utilizing silicon carbide (SiC) MOSFETs. Models EMI noise sources in the time domain under varying voltage and current conditions, enabling accurate EMI prediction and compliance with EMI standard.
	[128]	Introducing an enhanced method for analyzing parasitic elements in high-performance silicon carbide (SiC) power modules. The study accurately characterizes parasitic impedances, leading to improved design and performance of SiC power modules.
	[129]	Evaluating high-power silicon carbide MOSFET modules against silicon insulated-gate bipolar transistor modules. Highlights SiC MOSFETs' superior voltage blocking and faster switching capabilities, which enhance efficiency and performance.
	[130]	Presenting a switching loss model for silicon carbide (SiC) power MOSFETs, incorporating parasitic components to predict losses in high-frequency applications. The model validation accounts for the discharge and charge of the output capacitance.
	[131]	Studying and assessing the performance of an advanced neutral-point-clamped (ANPC) converter configuration comprising two SiC MOSFETs and four Si IGBTs per phase leg, focusing on high switching frequency operations.
	[132]	Investigating the integration of wide bandgap (WBG) devices into the DC/DC converters of EVs. A comprehensive model is developed to compare WBG-based converters with traditional silicon counterparts, highlighting performance improvements in EV applications.
	[133]	Examining the efficiency gains of integrating silicon carbide (SiC) MOSFETs into traction inverters for urban e-buses. Evaluates whether these efficiency improvements can offset the higher costs of SiC devices, providing insights into the economic viability of adopting SiC technology in e-transportation. According to the study, significant energy savings can be gained when the vehicle operates mostly in the partial load area.
	[134]	Carrying out a simulation and measurement-based analysis of efficiency improvements achieved by retrofitting a 400 V, 300 kW automotive traction inverter with SiC MOSFETs. The results refer to a considerable reduction in inverter power losses by approximately 50% compared to traditional silicon IGBT-based counterpart.

Table 8. *Cont.*

Main Area	Ref.	Core Contribution
Performance Analysis	[135]	Developing an analytical model to assess voltage distortions in SiC-MOSFET-based inverters for EVs, considering factors like voltage drops, dead time, and switching delays. Experimental results indicate that SiC-based systems exhibit lower voltage distortion and higher efficiency compared to traditional Si IGBT-based scheme.
	[136]	Performance assessment of GaN devices in an e-traction drive system for electric vehicles. The study demonstrates that GaN-based inverters enhance efficiency and dynamic response compared to traditional Si-based inverters.
	[137]	Holding comparison of power and energy losses in three-phase inverters using two SiC-MOSFET modules and one Si (Si-IGBT) module. It considers factors like blanking time and reverse conduction and thermal feedback drive cycles.
	[138]	Providing a comprehensive overview of applying finite element analysis (FEA) to the packaging of SiC power devices, addressing how (FEA) can be utilized to simulate and optimize the thermal, mechanical, and electrical performance of SiC power modules.

Table 9. Research contributions related to system design of WBG-based systems.

Main Area	Ref.	Core Contribution
System Design and Performance Improvement	[108]	Providing a comprehensive review of thermal design strategies for SiC power modules in EV motor drives. It emphasizes innovative heat sink optimization techniques and advanced simulation methods to enhance heat dissipation.
	[112]	Developing a highly integrated dv/dt filter design for silicon carbide (SiC) inverters, combining inductors, capacitors, and damping resistors directly into the bus bars. This approach reduces filter size and weight while maintaining compliance with NEMA standards, providing efficient motor protection against high dv/dt transients and voltage overshoots.
	[113]	Holding comparison of 2L SiC MOSFET and 3L Si IGBT (NPC and T-NPC) inverters for high-speed drives with long cables. Evaluates efficiency, overvoltage, heat sink design, and cost under same conditions. Addresses the trade-offs between SiC's high efficiency at low power and IGBT's cost-effectiveness advantage.
	[116]	Design and implementation of a Si/SiC hybrid five-level active neutral point clamped inverter for electric aircraft propulsion. Combines low-frequency Si switches and high-frequency SiC devices. A high-performance hybrid modulation strategy is verified experimentally.
	[121]	Introducing a soft-switching voltage slew-rate profiling approach for SiC-based motor drives to mitigate motor overvoltage caused by the reflected wave phenomenon. By optimizing the rise/fall time of the output voltage to match the cable anti-resonance period, motor overvoltage is eliminated.
	[122]	Developing a multi-conductor transmission line model to identify significant stress near the neutral point. Help mitigate insulation failure by managing anti-resonance effects in motor designs.
	[123]	Providing design and implementation of a 500 kW air-cooled silicon carbide (SiC) three-phase inverter. Achieves a record-breaking power density of 1.246 MW/m^3 and efficiency of 98.74%.
	[124]	Introducing a high-efficiency energy conversion system topology for 100 kW DC–DC power conversion using a 3.3 kV SiC device, achieving over 99.7% efficiency.
	[139]	Presenting a compact power module that combines Si IGBTs and SiC MOSFETs. The paper provides detailed gate driver designs and packaging solutions, offering guidelines for application-specific implementations.

Table 9. *Cont.*

Main Area	Ref.	Core Contribution
System Design and Performance Improvement	[140]	Addressing the challenge of motor overvoltage oscillations in silicon carbide (SiC)-based motor drives. A quasi-three-level PWM scheme is proposed. This technique allows voltage reflections along the cable to settle before the voltage reaches its final value, eliminating motor overvoltage oscillations in cable-fed drives.
	[141]	Proposing a cost-effective packaging methodology for high-power SiC intelligent power modules (IPMs) by repacking discrete SiC devices, aiming to meet the growing demand for high-current SiC power modules in EV applications.
	[142]	Introducing an optimized dead-time adjustment method for inverters utilizing an enhanced switching model of GaN-High Electron Mobility Transistors, reducing power losses and enhancing inverter efficiency.
	[143]	Presenting a SiC-based battery charger for plug-in EVs. The design attenuates the second order ripple power, enabling the use of smaller DC–link capacitors, reducing the system volume and cost.
	[144]	Investigating a design methodology for inverter-side resistor–inductor (RL) filters aimed at mitigating motor overvoltage in SiC-based drives. The employed approach effectively addresses issues arising from impedance mismatches between inverters and motors.
	[145]	Developing a 10 kV SiC-MOSFET power module. This configuration reduces parasitic inductances and capacitances, leading to a 53% increase in partial discharge inception voltage and a 90% reduction in common-mode current, enhancing high-voltage performance.
	[146]	Presenting a method to achieve zero switching loss in SiC MOSFETs by employing zero-voltage switching (ZVS), thereby minimizing thermal limitations, and enabling operation at higher switching frequencies.
	[147]	Designing a system-level tool that optimizes the power density of three-phase, two-level SiC-based inverters. The developed design tool predicts a 159% power density increase over Si-based inverters.
	[148]	Investigating the integration of (WBG) semiconductor devices, into renewable energy systems and smart grids. Some circuit design requirements to maximize the advantages of (WBG) have been addressed. Moreover, the merits such as efficiency and power density enhancement have been discussed as well.
	[149]	Addressing crosstalk and voltage oscillations in SiC MOSFET half-bridge converters by proposing a gate driver that generates a negative turn-off voltage without a negative power supply. Presents a simple snubber circuit to suppress the parasitic ringing. The findings confirm the effectiveness of the presented solutions to enhance the converter performance.
	[150]	Designing a high-power converter based on an SiC device, reducing conduction losses, and enhances efficiency, which is suitable for applications requiring compact and efficient power conversion solutions.
	[151]	Investigating a half-bridge gate driver circuit for SiC MOSFETs. The topology significantly reduces the total switching power losses by approximately 55% compared to conventional voltage source gate drivers, enhancing the converter efficiency.
	[152]	Introducing an inductor-less dv/dt filter for 100 kW to 1 MW voltage source converters using SiC devices. The design eliminates bulky filter inductors.
	[153]	Presenting a design methodology for dv/dt filters tailored to SiC-based inverters in high-frequency motor-drive systems. Thermal and electrical constraints have been addressed to mitigate insulation stress on motor stator windings caused by high slew rates in line voltages.

Table 9. *Cont.*

Main Area	Ref.	Core Contribution
System Design and Performance Improvement	[154]	Exploring the integration of WBG semiconductors, specifically into variable speed drive inverters. Introduces a soft-switching modulation scheme. The study also evaluates low-voltage GaN devices in multi-level inverter structures to enhance overall efficiency.
	[155]	Introducing a high-efficiency, high-power density On Board Chargers (OBCs) based on WBG devices. The design achieves reduced size, and lower electromagnetic interference (EMI), making it suitable for next-generation EV charging systems.
	[156]	Presenting high-performance GaN power transistors characterized by higher breakdown voltage and current density. The design improves the thermal performance and device scalability. Addresses the major limitations of GaN devices.
	[157]	Proposing a variable frequency control strategy and optimized filter design for SiC-based wind inverters. The approach maximizes energy extraction while minimizing switching losses. The method enhances the performance by dynamically adjusting the inverter's operating frequency.
	[158]	Developing a reduced power losses inverter system using lower harmonic loss technology and ultra-compact inverters using SiC modules. The system reduces harmonic distortion, minimizes power losses, and permits higher power density. The weight of the developed SiC-based inverter has been reduced by 55% of a conventional IGBT inverter.
	[159]	Designing a current–source inverter (CSI)-integrated motor drive utilizing dual-gate four-quadrant (WBG) power switches. This design enables bidirectional power flow, reduced switching losses, and enhanced system efficiency. The approach offers a compact, high-performance solution for next-generation motor drive systems.

Table 10. Research contributions related to cooling systems of WBG-based systems.

Main Area	Ref.	Core Contribution
Thermal Management and Cooling Systems	[160]	Developing a cost-effective, 3D-printed heatsink for rapid prototyping of WBG power converters. The design enables faster development cycles, reduces prototyping costs, and enhances thermal management in industrial and automotive applications.
	[161]	Investigating a cooling system for automotive SiC power modules using a modular manifold with an embedded heat sink. This design improves thermal management, reduces system size, and enhances cooling efficiency.
	[162]	Proposing a cooling system for SiC traction inverters in EVs using heat pipes. This design enhances thermal dissipation, reduces temperature fluctuations, and improves inverter reliability and power density.
	[163]	Investigating cooling techniques and enclosure designs for integrated motor drives (IMDs). Evaluates various cooling methods, including liquid- and air-based systems, to optimize thermal management and enhance drive performance.
	[164]	Carrying out a thermal analysis of housing-cooled integrated motor drives (IMDs). The study examines the heat dissipation performance of housing-based cooling systems, highlighting design factors that improve thermal management. Their approach enables more compact, efficient, and reliable IMD designs.
	[165]	Developing a cooling design tool for EV SiC inverters using transient 3D-CFD simulations. The tool optimizes thermal performance by predicting heat dissipation and fluid flow dynamics. This approach enhances inverter cooling efficiency and reduces system size.

Table 10. *Cont.*

Main Area	Ref.	Core Contribution
Thermal Management and Cooling Systems	[166]	Presenting a comprehensive review of cooling concepts and thermal management techniques for automotive WBG inverters. Categorizes cooling topologies, technologies, and integration strategies.
	[167]	Proposing a design methodology of air-cooled SiC inverters employed in EVs, optimizing thermal management, power density. The paper enables compact, efficient, and cost-effective SiC inverters.
	[168]	Presenting an optimal design of an integrated heat pipe air-cooled system for SiC MOSFET converters using the teaching–learning-based optimization algorithm. Their approach enhances thermal performance, minimizes cooling system size, and improves converter efficiency.
	[169]	Presenting an automated methodology for designing and optimizing air-cooled heatsinks for SiC power modules. Integrates genetic algorithms with finite element analysis. Complex heatsink geometries have been generated with this approach. The findings indicate that the size of the optimized heatsink is less than the conventional design approach by 27%; meanwhile, the resultant junction temperature is reduced by 6%.
	[170]	Introducing a thermal management design methodology for SiC power devices and systems using genetic optimization algorithms to achieve optimum geometries for liquid-cooled heat sink. This approach enables the creation of effective complex cooling structures for power electronic systems.
	[171]	Proposing a design optimization method for liquid-cooled heat sinks in WBG power modules, utilizing Fourier analysis and evolutionary multi-objective optimization. The developed heat sinks with this approach outperforms the conventional heat sinks shapes.
	[172]	Presenting a double-sided cooling method for discrete SiC MOSFETs using a press-pack package. This approach enhances thermal dissipation, enabling higher power density and reducing thermal stress. The design achieves improved heat distribution and increased device reliability.
	[173]	Investigating the performance of SiC and GaN devices under cryogenic cooling. The findings indicate that SiC MOSFETs have relatively greater on-state resistance and relatively slower switching speeds at low temperatures, while GaN devices demonstrate improved performance.
	[174]	Investigating a design of a power electronics package that integrates different materials. The design improves thermal cycling reliability of liquid-cooled aluminum SiC heat sinks. The proposed structure and layers minimize the coefficient of thermal expansion mismatch in the stack by 84%, extending the lifetime of the package and permits reduction in the volume and weight.
	[175]	Presenting thermal analysis and material selection methodology for SiC-based Intelligent Power Modules (IPMs). By evaluating various materials and their thermal properties, the study aims to enhance the thermal performance and reliability of SiC IPMs.
	[176]	Designing a thermally uniform heatsink for high-power SiC inverters employed in EVs. A novel heatsink geometry that improves cooling efficiency and thermal uniformity is presented.
	[177]	Investigating a thermal modeling and simulation method for optimizing power density in SiC-MOSFET inverters. The proposed approach allows for optimal placement and design of power modules, optimizing the volume and compactness of the SiC-MOSFET inverter.
	[178]	Proposing an optimal thermal design for SiC power modules. A double-sided cooling strategy to enhance heat dissipation and thermal uniformity is presented. Compact and reliable SiC-based power modules for high-voltage applications can be achieved.

Table 10. *Cont.*

Main Area	Ref.	Core Contribution
Thermal Management and Cooling Systems	[179]	Introducing a liquid cooling method for SiC power modules. The proposed method is based on direct liquid contact with the surface of the power module, enhancing thermal dissipation and reducing thermal resistance.
	[180]	Presenting a passive cooling system for high-power SiC power electronic converters. The proposed heat sink enhances heat dissipation and thermal uniformity using phase-change heat transfer. The presented cooling system results in reduced thermal resistance, improving the cooling efficiency.
	[181]	Proposing cooling strategies and thermal management methods for WBG-based current–source inverters (CSIs) employed in motor drives. With the proposed approach, the system compactness is enhanced.
	[182]	Investigating a thermal design methodology for WBG inverters. An optimized cooling structure is proposed. The developed design improves heat dissipation and increases the reliability of WBG inverters.

Table 11. Research contributions related to key challenges and solutions of WBG-based systems.

Main Area	Ref.	Core Contribution
Key Challenges and Solutions	[183]	Presenting a review including key challenges and solutions for GaN power semiconductor modules. Advancements in GaN technology has been addressed. The paper discusses the main challenges such as parasitic effects, and thermal stress. Some proposed solutions have been addressed as well.
	[184,185]	Providing a review on the key advancements, challenges, and future trends in WBG semiconductor technologies for modern automotive and renewable energy systems. Innovations in device design and fabrication technologies have been addressed.
	[186]	Highlighting the superior performance of WBG devices in power electronic converters. Presents some design methodologies and addresses key challenges like parasitic effects and thermal stress.
	[187]	Addressing advancements in WBG devices for the automotive industry. Items such as power density, efficiency, and thermal performance, have been discussed. Moreover, main challenges, including cost, reliability, and integration, are also presented.
	[188]	Discussing the main challenges that affect the reliability and performance of SiC and GaN power semiconductor devices. The article suggests a roadmap for enhancing the quality and reliability of WBG devices for next generation power electronic converters.
	[189]	Reviewing the reliability challenges and packaging of WBG devices. The article provides information about improving the devices' lifespan and durability for various applications.
	[190]	Investigating the potential of WBG in power electronics. Highlights their superior efficiency, higher switching frequencies, and elevated temperature operation compared to silicon-based devices. Main challenges have been addressed as well.
	[191]	Providing a review of packaging technologies and challenges of SiC power modules, like high-speed switching, thermal management, high-temperature operation, and high-voltage isolation. Discusses emerging issues in soft-switching converters and low-temperature applications of SiC devices.
	[192]	Addressing switching oscillations in WBG semiconductor devices. Classifies oscillation types, analyzes their causes and effects. Suppression techniques have been presented to enhance the performance and reliability of WBG-based power electronic converters.

Table 11. *Cont.*

Main Area	Ref.	Core Contribution
Key Challenges and Solutions	[193]	Investigating the integration of CMOS logic with WBG and ultra-WBG semiconductors. The article identifies challenges such as material defects and fabrication complexities. Also presents directions and guidelines to overcome these challenges.
	[194]	Discussing the potential of WBG power semiconductor devices. Presents the International Technology Roadmap for WBG devices, highlighting the challenges and strategies for accelerating adoption and commercial acceptance of WBG-based devices and converters.
	[195]	Addressing advancements in WBG semiconductors. The paper outlines the programs of U.S. Department of Energy that have fostered the innovations through the value chain of power electronics.
	[196]	Presenting the major application of SiC power devices. The article addresses the main obstacles such as the crosstalk effects, current overshoot, and electromagnetic interference. Also presents the possible solutions to alleviate the adverse effects of such obstacles.
	[197]	Providing a review of employment of wide bandgap (WBG) power semiconductor modules in EVs. Main design aspects such as die parallelization and Direct Bonded Copper (DBC) routing have been discussed to enhance efficiency and performance of EV drives.
	[198]	Designing of 30 kVA three-phase SiC-MOSFETs inverter that can operate at ambient temperatures up to 180 °C. Key challenges of operation at such high-temperature have been addressed. The findings prove that SiC-based inverters are feasible in harsh environments.
	[199]	Investigating the obstacles that prevent widespread and adoption of WBG semiconductors in power electronics applications. The main challenges like material defects and high manufacturing costs have been discussed. Some solutions have been addressed to overcome such challenges.
	[200]	Discussing the application and advantages of SiC power devices. The paper discusses challenges and suggest solutions to enhance the performance of SiC devices.
	[201]	Providing a comprehensive review of methods for suppressing conductive common-mode electromagnetic interference in inverter-fed motor drives. The paper also discusses the impact of emerging WBG devices on EMI.
	[202]	Designing an inverter for EV based on double-sided cooled SiC power modules. This method enhances thermal management and increases the power densities, thereby contributing higher reliability and compactness of the inverter.
	[203]	Addressing the characteristics and commercial status of GaN power devices, highlighting their potential for higher frequency and efficiency in power electronic converters compared to conventional Si devices. Also discusses some challenges such as gate driver design, unique reverse conduction behavior, and breakdown mechanisms of the device.

Moreover, state-of-the-art ratings and main manufacturers of SiC-Base MOSFET power transistors, as one of the WBG power semiconductor devices, are summarized in Table 12.

Owing to Ref. [204], typical state-of-the-art ratings and main manufacturers of SiC power transistors, as one of the WBG power semiconductor devices, are summarized in Table 12.

Table 12. Typical ratings and some manufacturers of SiC power MOSFETs.

Manufacturer	Voltage Rating [V]	Current Rating [A]
ST Microelectronics, Switzerland	600–2200	7–300
Infineon, Germany	400–2000	5.2–238
Semikrone, Germany	1200–1700	18–485
Microchip, USA	700–3300	6–149
IXYS, USA	900–1700	3.5–142
Mitsubishi, Japan	1200–1700	100–1200
Toshiba, Japan	650–1200	20–100
Alfa and Omega, USA	650–1200	6.3–96
Solitron, USA	650–1200	40–120
WeEn, China	650–1700	4.6–216

Reference [204] Available online: https://us.metoree.com/categories/sic-mosfet/ (accessed on 15 December 2024).

4. Main Control Techniques of IM Drives

4.1. Introduction

The most used control techniques applied in industrial IM drives are field-oriented control (FOC) and direct torque control (DTC). FOC, originated by Blaschke in [205], is utilized in IM drives when a precise speed and a high dynamic response are required [206–223].

A few decades after inventing FOC, the direct torque control (DTC) technique was proposed by the authors of [12] to provide fast dynamic response and good control of both motor flux and electromagnetic torque [224–239]. The first industrial DTC-based IM drive was designed and fabricated by ABB in 1996, introduced in [240].

On the other hand, many research activities have been conducted recently aiming to employ the finite control set model predictive control (FCS-MPC) approach to regulate motor speed, torque, and flux based on the dynamic model of the IM.

Moreover, for high-efficiency IM drives, the core control algorithms can involve efficiency optimization task/subroutine (function) to minimize the energy consumption by operating at optimum levels of flux and minimizing the reactive component of the current drawn from the AC supply. Also, adopting regenerative braking approach enhances the overall efficiency of the AC drive by returning to the grid the mechanical energy stored in the motor shaft during braking instants.

4.2. Field-Oriented Control

The commonly used and well-known scalar control methods of IMs provide satisfactory steady performance for economic general purpose AC drives. However, they are neither able to provide high transient response, nor are they suitable for precise operation and applications at low and very low speeds. In addition, scalar methods fail to achieve position control of IMs as servo drives. The field-oriented control, or vector control (VC), technique for IM drives was developed to overcome the main limitations of the scalar control methods

The FOC, or VC, technique aims to emulate the decoupled control features of a conventional separately excited DC motor by decomposing the stator current vector into two orthogonal components: direct component I_d and quadrature component I_q. The direct component I_d is responsible for air gap flux production, while the quadrature component I_q is responsible for electromagnetic torque production, as illustrated in Figure 7. This way, the FOC emulates the behavior of the DC motor, which results in high dynamic

performance and good transient response under sudden load variations, provided that the machine parameters are identified on-line during the motor operation.

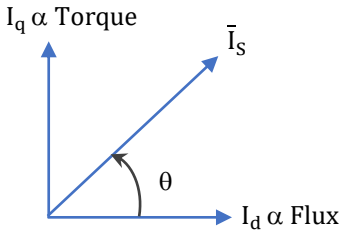


Figure 7. Phasor diagram of stator current components with FOC.

The block diagram of the basic scheme of FOC of IM drives is presented in Figure 8.

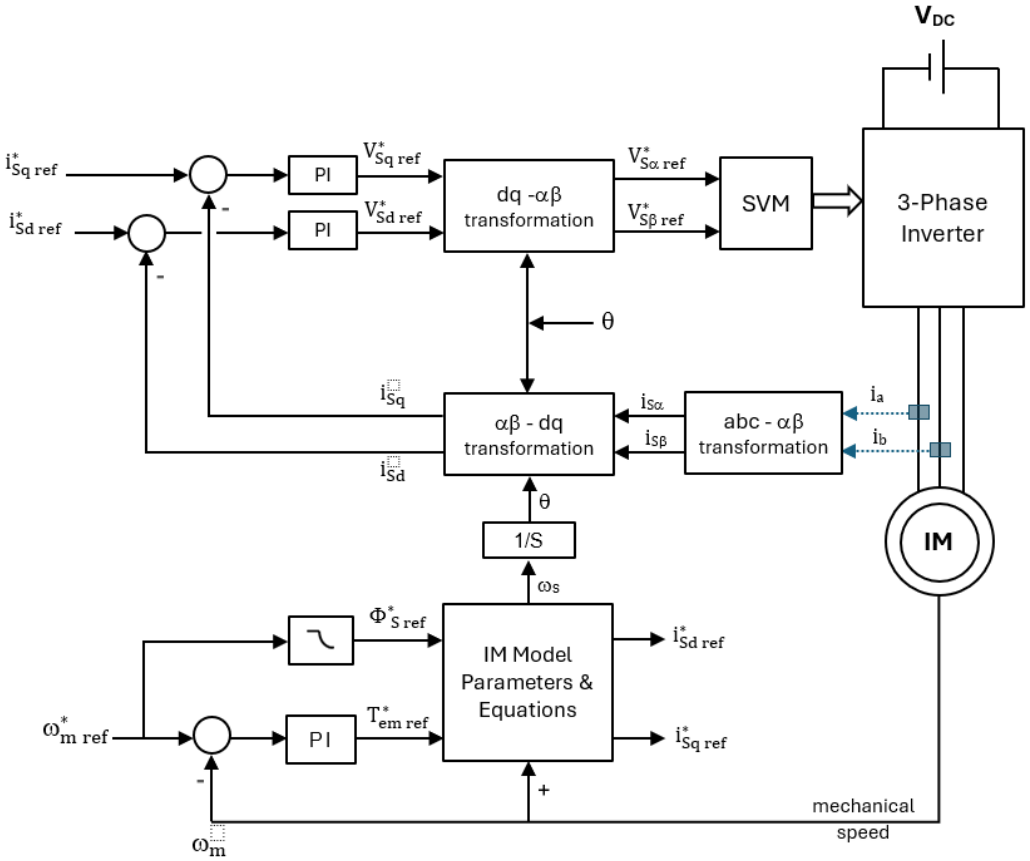


Figure 8. Block diagram of the basic scheme of FOC of IM drives.

In the VC or FOC system of 3-Φ IM, the reference electromagnetic torque T^*_{emref} is computed as the output of the PI-speed controller. The reference stator flux F^*_{Sref} is a function of the reference speed, involving the operation in the field weakening mode for motor operation at speeds above the rated value, as illustrated in the lower part of Figure 8.

Meanwhile, the reference stator currents i^*_{Sdref} and i^*_{Sqref} in the d-q coordinates are generated with the aid of IM parameters owing to the model equations given below:

$$i^*_{Sd\ ref} = \frac{\Phi^*_{S\ ref}}{L_S} \quad (1)$$

$$i^*_{Sq\ ref} = \frac{4}{3}\frac{T^*_{em\ ref}}{P\Phi^*_{S\ ref}} \quad (2)$$

These equations are based on the following assumptions:

1. The stator flux linkage is typically aligned along the d-axis, and the q-axis flux component is zero. Accordingly: $\Phi^*_{Sd} = \Phi^*_{S\ ref}$; $\Phi^*_{Sq} = 0$;
2. The reference stator current in the d-axis is directly related to the stator flux linkage;
3. The rotor is short circuited, where: $V_{rd} = V_{rd} = 0$.

The electromagnetic torque is computed using the following equation:

$$T_{em} = \frac{3}{2}\frac{P}{2}\left(\Phi_{Sd} i_{Sq} - \Phi_{Sq} i_{Sd}\right) \quad (3)$$

The slip speed is determined using the following relation:

$$\omega_{slip} = \frac{R_r}{L_r}\frac{i_{Sq}}{i_{Sd}} \quad (4)$$

$$\omega_s = \omega_{slip} + \omega_m \quad (5)$$

where T^*_{em} is the reference electromagnetic torque (Nm); T_{em} is the instantaneous electromagnetic torque (Nm); Φ_{Sd} and Φ_{Sq} are the stator flux components in d-q synchronous reference frame (Wb); i_{Sd} and i_{Sq} are the stator current components of stator current in d-q synchronous frame (A); ω_s is the synchronous speed (rad/s); ω_{slip} is the slip speed (rad/s); ω_m is the motor mechanical speed (rad/s); P is the number of poles; L_s is the stator self-inductance (H); L_r is the rotor self-inductance (H); R_r is the rotor resistance (W); and L_r is the rotor self-inductance (H).

Although the FOC provides good transient performance of the IM, it suffers from several drawbacks. Firstly, the successful operation depends on the accuracy of estimation (computation) of slip speed (ω_{slip}) and the angle (q), which depend on the rotor time constant (L_r/R_r) that varies with the temperature and level of saturation.

In fact, considerable research efforts have been done in VC and FOC of IM during the period of 1992–2008, with the advancement in DPS and microcontroller technologies. However, the main observed research contributions of FOC of IM drives during the period of 2017 to 2024 are summarized and presented in Table 13.

Table 13. Research contributions in FOC of induction motor drives.

Main Area	Ref.	Core Contribution
FOC	[205]	Proposing and explaining the principle of field orientation (FO) for controlling rotating-field machines, such as IMs. Pioneer work in the field of vector control (VC) of AC motors.
	[206]	Presenting a sensorless (FOC) strategy for IMs for submarine pumps. Motor speed and flux are estimated using electrical measurements, enhancing the system reliability by eliminating the need for deep-sea sensors.
	[207]	Investigating discrete-time direct and indirect FOCs in stationary reference frame for IMs. Accurate tracking of torque and flux references have been developed.
	[208]	Introducing a space vector modulation (SVM) technique for distributed inverter-fed IM drives for EVs. This method optimizes voltage utilization and minimizes harmonic distortion. Drive reliability and overall efficiency have been improved.
	[209]	Addressing the challenges of accurate flux estimation in FOC of IMs, under parameter detuning. A flux observer based on the Gopinath model has been proposed, mitigating issues such as saturation of integrators. With the proposed method, the flux estimation accuracy is enhanced.
	[210]	Presenting a genetic algorithm-hybrid fuzzy controller for speed control of IMs drives based on SVPWM. Simulation and experimental results indicate enhanced performance under various operating conditions.

Table 13. *Cont.*

Main Area	Ref.	Core Contribution
FOC	[211]	Proposing a fault-tolerant control strategy for rotor FO of IM drives. The method dynamically adds a common-mode voltage to the reference phase voltages relying on motor load conditions. Maintains torque and speed during post-fault operations.
	[212]	Investigating an indirect rotor FO control technique for IM drives operating under an open-phase fault. The method manages the unbalanced conditions caused by the fault.
	[213]	Proposing an improved nonlinear flux observer for a sensorless-FOC of IM drive. The system involves an adaptive predictive current control to enhance dynamic performance and robustness under parameter variations. The method improves torque control and provides faster transient response.
	[214]	Investigating a modified FOC strategy with optimal rotor flux for fault-tolerant control of IM Drives operating under single-phase open fault conditions. The employed method ensures torque ripple reduction and continuous operation.
	[215]	Presenting a FOC strategy for multiphase drives. The approach maintains drive operation under phase faults without reconfiguration; stable torque production and reduced ripple are guaranteed. This method is suitable for critical applications that requires continuous operation under fault condition.
	[216]	Investigating application notes of typical FOC of IMs by decomposing stator currents into two orthogonal components: one governing magnetic flux and the other controlling torque.
	[217]	Proposing a PI observer with a reduced order integrating unit for IM drive control. The method reduces computations complexity and improves robustness against parameter variations. Accurate speed and flux estimation have been achieved.
	[218]	Providing a review of advanced control strategies for IMs focusing on field-oriented control (FOC), direct torque control (DTC), and model predictive control (MPC). The paper presents the principles of operations, main advantages, and limitations.
	[219]	Proposing a Model Reference Adaptive System (MRAS)-based switching linear feedback strategy for sensorless speed control of IM drives. The approach enhances the accuracy of speed estimation and robustness against parameter variations. The method permits successful sensorless control of IM drives.
	[220]	Investigating a MRAS using rotor flux space vectors for FOC of IM drives. The MRAS enhances rotor flux estimation accuracy, ensuring precise speed estimation under parameter variations. The method reduces steady-state error and enhances dynamic performance.
	[221]	Presenting a sensorless control strategy for IM drive using a stator voltage MRAS for EVs. The method ensures accurate speed estimation at low speeds, enhancing system reliability during sensor failure.
	[222]	Proposing a sensorless-FOC system for five-phase IM with real-time parameter estimation. The approach enhances speed and flux estimation accuracy while compensating for parameter variations. Involving the parameter estimation into the control loop results in a high-performance sensorless IM drive.
	[223]	Implementing a real-time indirect rotor flux oriented control (IRFOC) for a five-phase IM. A Sliding Mode Observer is employed for rotor resistance adaptation. The method enhances speed and flux estimation accuracy under varying rotor resistance.

4.3. Direct Torque Control

DTC strategy of IM drives controls directly both stator flux and electromagnetic torque by applying instantaneously the optimum inverter switching state which satisfy both torque and flux requirements. Owing to Figure 9, the DTC scheme of 3-Φ IM is composed of the following blocks:

1. Motor transient model to calculate the instantaneous value of the stator flux vector and electromagnetic torque.
2. Two hysteresis ON/OFF controllers: one for the stator flux and the other for the torque.

3. Optimum switching table whose output is the instantaneous values of the inverter switching state, such that the flux and torque track the set points (reference values).

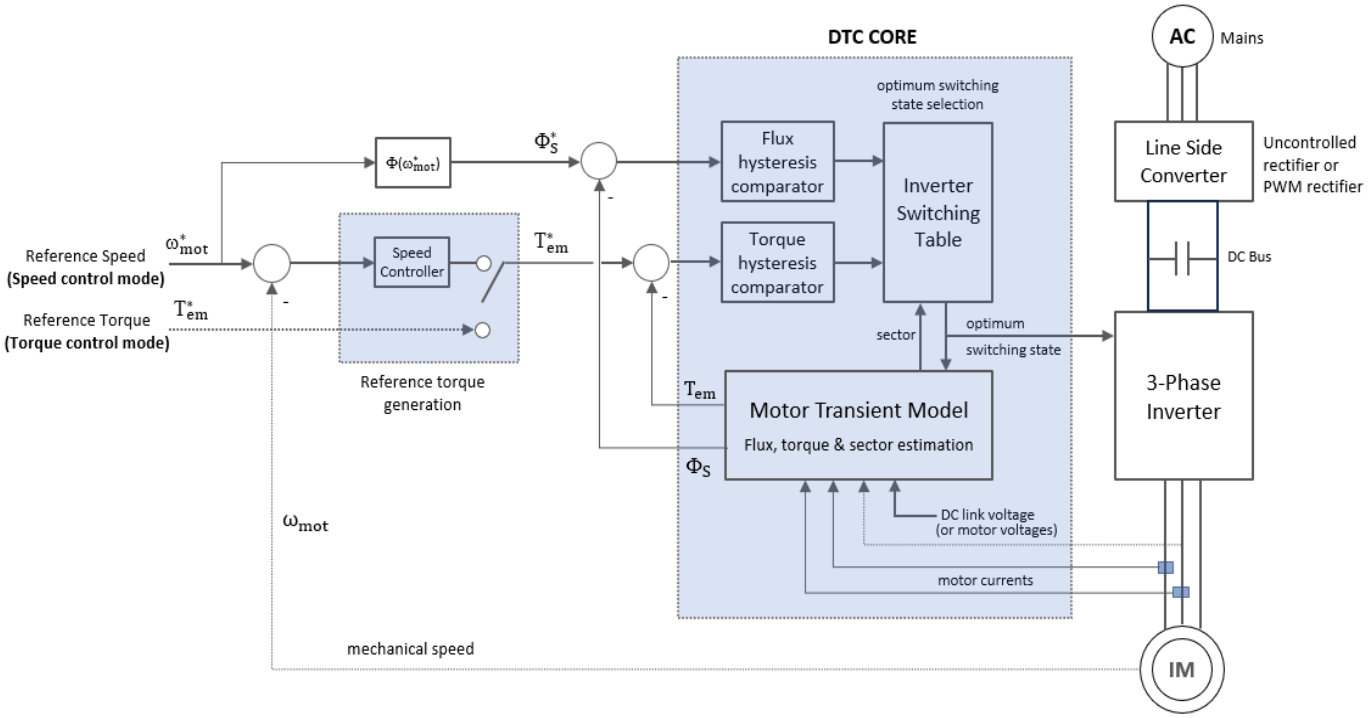


Figure 9. Block diagram of a conventional DTC system of an IM drive.

The DTC strategy of IM drive can have two modes of operation: torque control mode and speed control mode. In torque control mode, the desired electromagnetic torque is the reference signal. In speed control mode, the reference torque is the output of speed controller. The reference flux signal is a function of the motor reference speed. For speeds greater than the rated value, the reference stator flux is reduced, running the motor in field weakening mode. The flux and torque control under DTC can be explained with the aid of Figures 10 and 11, respectively, where the stator flux vector initially lies in sector number one. Each discrete inverter switching state and the corresponding voltage vector has its effect on both electromagnetic torque and stator flux; e.g., if the voltage vector V_1 is applied during the sampling period, the magnitude of the stator flux will increase. At the same time, the angle between stator and rotor flux vectors will decrease, which results in a reduction in the instantaneous value of the electromagnetic torque. From the principles of electric machines, the magnitude of the electromagnetic torque is directly proportional to the SINE value of the angle between stator and rotor flux vectors.

Applying vector V_4 instead of V_1 results in a reduction in magnitude of stator flux, as illustrated in Figure 10. At the same time, the angle between stator and rotor flux vectors will increase, which results in an increment in the instantaneous value of the electromagnetic torque. From these observations, an optimum switching table is obtained to control simultaneously both stator flux and electromagnetic torque.

Figure 12 summarizes the effects of all inverter voltage vectors on both torque and flux in Sector 1.

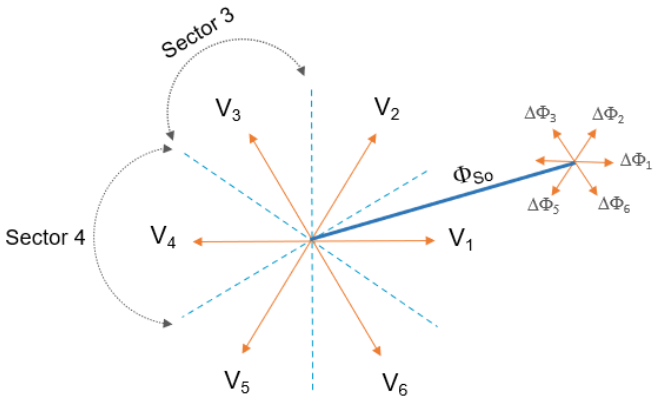


Figure 10. Stator flux vector lies in Sector 1.

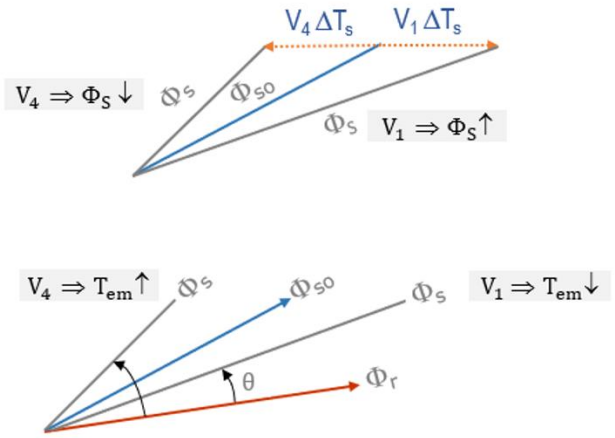


Figure 11. Control of motor stator flux and torque in Sector 1.

Sector 1		
Vector	ΔΦs	ΔTe
V1	++	-
V2	+	+
V3	-	++
V4	--	+
V5	-	-
V6	+	--
V0, V7	0	-

Note: ++ high positive variation; + moderate positive variation; -- high negative variation; - moderate negative variation

Figure 12. Effects of inverter discrete voltage vectors on stator flux and torque in Sector 1.

The ideal trajectory of the stator flux vector is a circular path. Under DTC strategy, the actual path is formed by applying instantaneously the optimum inverter voltage vectors. Such optimum vectors depend on both the current location of the stator flux vector (Sector number 1:6) and the direction of rotation as well.

Figure 13 clarifies and indicates the selection method of the optimum inverter vectors in Sectors ONE and TWO, where:

For CCW rotation in Sector ONE, vectors V_2 and V_3 are to be mutually applied to follow the desired flux trajectory; while in Sector TWO, vectors V_3 and V_4 are to be mutually applied to follow up the required stator flux trajectory.

For CW rotation in Sector ONE, vectors V_5 and V_6 are to be mutually applied to keep track of the desired flux locus; while in Sector TWO, vectors V_1 and V_6 are to be mutually applied in Sector TWO.

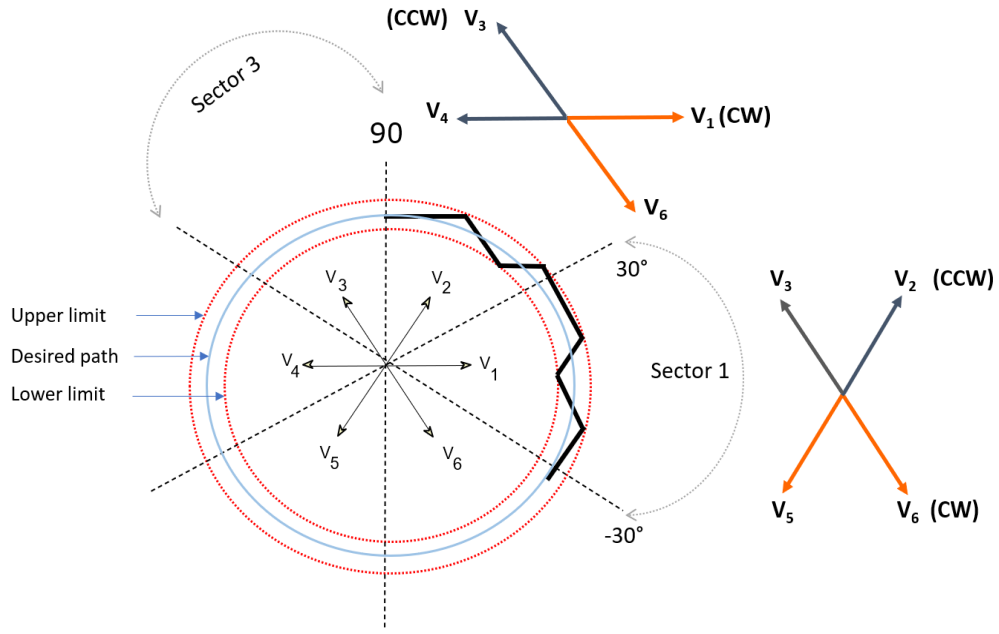


Figure 13. Trajectory of stator flux vector under DTC with conventional two-level VSI.

The stator flux components in the (α–β) stationary reference frame are computed using the following equations:

$$\overline{\Phi}_S = \Phi_\alpha + j\Phi_\beta \tag{6}$$

$$\Phi_\alpha = \int_0^{T_S} (v_\alpha - R_S i_\alpha)dt \tag{7}$$

$$\Phi_\beta = \int_0^{T_S} (v_\beta - R_S i_\beta)dt \tag{8}$$

where T_S is the sampling period of the DTC algorithm in digital implementation.

The magnitude and the location of the stator flux vector are computed by Equations (9) and (10), respectively. They are inputs to the DTC blocks (hysteresis flux controller and the inverter switching table), as shown in Figure 9.

$$|\Phi_S| = \sqrt{\Phi_\alpha^2 + \Phi_\beta^2} \tag{9}$$

$$\Psi_S = \tan^{-1}\left(\frac{\Phi_\beta}{\Phi_\alpha}\right) \tag{10}$$

The electromagnetic torque produced by the IM is calculated using Equations (11) and (12):

$$T_{em} = \frac{3}{2}\frac{P}{2}(\overline{\Phi}_S \times \overline{I}_S) \tag{11}$$

$$T_{em} = \frac{3}{2}\frac{P}{2}(\Phi_\alpha i_\beta - \Phi_\beta i_\alpha) \tag{12}$$

where P is the number of magnetic poles of the AC motor.

The stator current components in the (α–β) stationary reference frame are determined using Equations (14) and (15):

$$\overline{I}_S = i_\alpha + ji_\beta \tag{13}$$

$$i_\alpha = \frac{1}{3}(2i_a - i_b - i_c) \quad (14)$$

$$i_\beta = \frac{1}{\sqrt{3}}(i_b - i_c) \quad (15)$$

The major advantages of DTC are the quick response of both torque and flux, as well as dependency of the DTC algorithm on a machine model with a moderate degree of complexity, unlike FOC, which is based on a sophisticated machine mode.

However, the main drawbacks of the DTC are the requirement of online identification of stator resistance to achieve high performance at low speeds, and the conventional scheme is not applicable for position control and servo applications.

In fact, considerable research activities in DTC drives have been carried out during the period of 1997–2017. The main observed research contributions of DTC for IM drives during the period of 2017 to 2024 are summarized and presented in Table 14.

Table 14. Research contributions in DTC technique of induction motor drives.

Main Area	Ref.	Core Contribution
DTC	[224]	Introducing an offline method to generate the optimum reference flux linkage in DTC scheme of IM drives. A lookup table based on nonlinear relations is constructed to determine the optimal flux linkage values corresponding to references speed and torque, thereby enhancing the efficiency of the motor for a wide speed range.
	[225]	Presenting a Modified Brain Emotional Controller to reduce torque and flux ripples in sensorless IM drives at low speeds. By emulating the rapid decision-making processes of the mammalian brain, the controller enhances the performance of the SVM-based DTC scheme. Experimental results indicate significant improvements in dynamic response.
	[226]	Proposing two control methods to enhance DTC of IMs using a Constant Frequency Torque Controller. These methods aim to improve torque dynamic performance. Adopting interleaving triangular carriers results in faster torque response and better flux regulation.
	[227]	Investigating a Dynamic Hysteresis Torque Band method for enhancing Lookup-Table-Based DTC of IMs. The method adjusts the torque hysteresis band based on flux error, improving torque response and reducing flux droop. This approach enhances steady-state and dynamic performance while maintaining the simplicity of conventional DTC scheme.
	[228]	Presenting a MRAS-based estimator for online stator resistance estimation in DTC of six-phase IMs. The proposed method enhances torque and flux estimation accuracy under varying temperature conditions.
	[229]	Providing a comprehensive review of advancements in DTC of IM drives. Examines various DTC strategies. Improvements in torque ripple reduction, switching frequency optimization, and sensorless control techniques have been addressed and discussed.
	[230]	Addressing the key advancements in DTC of IMs drives, in terms of reduction of torque and flux ripples, improving dynamic response, and minimizing dependency on motor parameters. Evaluates methods such as SVM, predictive control, and AI-based approaches, indicating benefits and limitations.
	[231]	Introducing a simplified DTC scheme for IM drives, integrating SVM with a single PI controller. The method reduces torque ripples and maintains a constant switching frequency, enhancing overall drive performance.
	[232]	Introducing a DTC scheme for IMs using synchronous PWM. This approach enhances torque ripple reduction and provides a control of switching frequency control.
	[233]	Proposing a DTC scheme of IMs employed in EVs, integrating Maximum Torque Per Amper to enhances energy efficiency. The scheme achieves superior drive performance.
	[234]	Developing a Full-Order Observer for DTC IM drive. This method improves rotor flux estimation accuracy and torque control, ensuring satisfactory stability for a wide speed range.
	[235]	Presenting a DTC scheme for IMs, integrating SVM with a Sliding Mode Controller. The scheme reduces torque ripple and improve system robustness against parameter variations, ensuring a high-performance drive.

Table 14. *Cont.*

Main Area	Ref.	Core Contribution
DTC	[236]	Proposing an adaptive DTC system for five-phase IMs using a Luenberger–Sliding Mode Observer (LSMO) for online stator resistance estimation. This method ensures system robustness against parameter variations, providing accurate torque and flux control.
	[237]	Introducing a sensorless DTC scheme for IMs, integrating Feedback Linearization with MRAS and Sliding Mode Observer for stator flux estimation. This approach eliminates speed sensors and enhances robustness against parameter variations.
	[238]	Proposing a DTC system for five-phase IMs, employing a Constant Switching Torque Controller and a Fractional-Order Proportional-Integral. The approach improves low-speed torque characteristics, minimizes torque ripple, and enhances system stability.
	[239]	Investigating a DTC scheme for IMs using a Minimum Voltage Vector Error approach. The method optimizes voltage vector selection and reduces torque ripples. Provides good dynamic response and enhances energy efficiency.
	[240]	Pioneer work developed by ABB as the first industrial DTC-based IM drive. DTC is an advanced method for controlling AC motors. In DTC, the motor torque and flux are controlled directly by selecting the optimal inverter switching state that satisfy both torque and flux reference values without the need for coordinate transformations and PWM unit.

4.4. Model Predictive Control

Recently, finite control set model predictive control (FCS-MPC) has been applied in IM drives as an advanced control approach [241–257] to minimize the torque and flux ripples and achieve other goals, such as minimization of switching frequency.

In the FCS-MPC technique, the future behaviors of the controlled variables (stator flux and electromagnetic torque in case of IM drives) are predicted for a finite time frame of one or more sampling period. Accordingly, the optimum future control action is applied to the motor to satisfy a customized goal function, where the FCS-MPC algorithm repeatedly checks the future behavior at every sampling period. Therefore, in addition to the main speed control (regulation) task, other goals can be achieved, such as minimization of flux and torque ripples, minimization of inverter switching frequency, minimization of stator current ripples, or minimization of active and reactive power ripples. Accordingly, the cost function can accommodate all these terms and more, owing to the performance requirement of the IM drive as demonstrated in Equations (16)–(19):

$$J_1 = \left|T_{em}^{*} - T_{em}^{k+1}\right| + \left|\Phi_S^{*} - \Phi_S^{k+1}\right| \tag{16}$$

$$J_2 = \left|T_{em}^{*} - T_{em}^{k+1}\right| + \left|\Phi_S^{*} - \Phi_S^{k+1}\right| \tag{17}$$

$$J_3 = \left|i_{S\alpha}^{*} - i_{S\alpha}^{k+1}\right| + \left|i_{S\beta}^{*} - i_{S\beta}^{k+1}\right| \tag{18}$$

$$J_{pq1} = \left|P_{ref} - P^{k+1}\right| + \left|Q_{ref} - Q^{k+1}\right| \tag{19}$$

The absolute value functions of the previous equations can be replaced by square functions for minimizing the terms of the formulated cost functions.

Moreover, each term can have a weight factor (w_p and w_q) to prioritize some term(s) during operation, as given by Equation (20):

$$J_{pq2} = w_p\left(P_{ref} - P^{k+1}\right)^2 + w_q\left(Q_{ref} - Q^{k+1}\right)^2 \tag{20}$$

The block diagram of FCS-MPC of IM drives is shown in Figure 14. The control system has three main parts:

1. Speed control loop and reference signals generation of torque and flux. The output of the PI speed controller represents the desired electromagnetic torque, while the reference stator flux is kept constant at the rated value for the entire range of speed from zero to the rated value. Above the rated value, the flux is reduced inversely to verify field weakening mode.
2. Computation of stator currents and stator voltages components in the (α–β) stationary reference frame.
3. FCS-MPC algorithm, which is composed of several blocks and functions, such as prediction of stator currents and stator flux components in the stationary reference frame (α–β) one sample ahead, and prediction of electromagnetic torque one sample ahead as well. Finally, in FCS-MPC, the customized cost function is calculated and checked for all inverter switching states. Then, the optimum inverter switching state that instantaneously provide minimum cost function is chosen and applied to the IM.

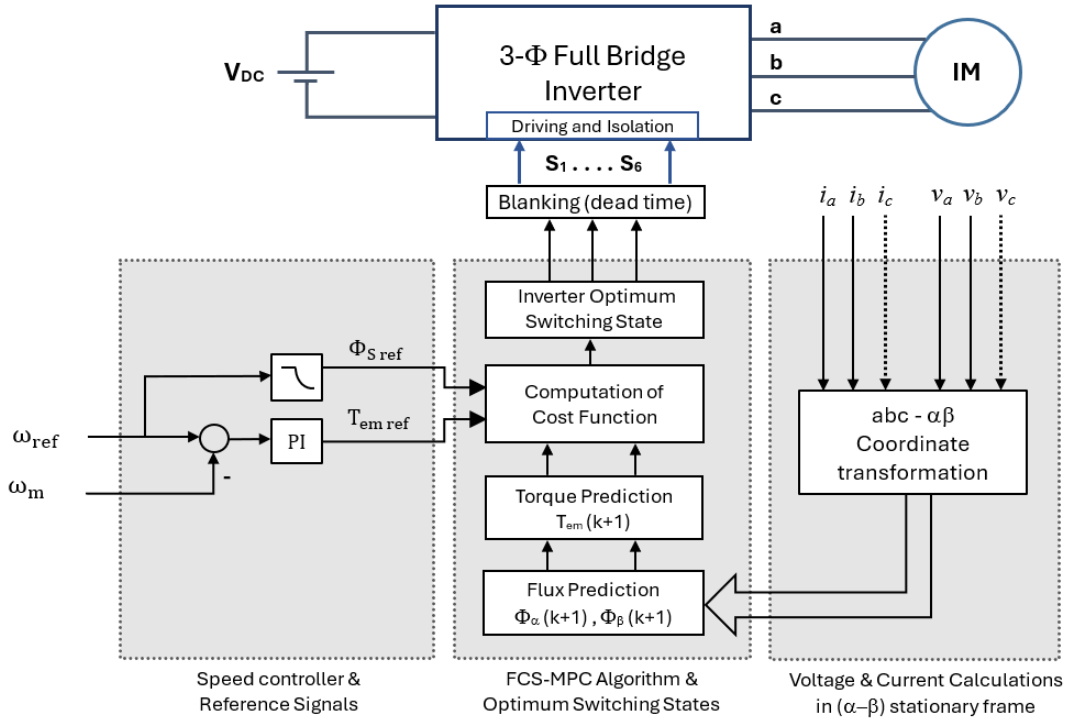


Figure 14. Block diagram of FCS-MPC system of IM drive.

The FCS-MPC approach requires a high-speed DSP unit to implement the several functions and subroutines related to the sophisticated algorithm. The accuracy of stator flux and electromagnetic torque prediction depends on the machine parameters plugged into the model. Thus, any deviation from the real values, which are affected by temperature and saturation level of the machine, negatively affects the performance of the IM drive, and maybe the stability as well.

Recently, several research efforts have been exerted in applying and investigating the IM drive under the FCS-MPC approach. The summary of main research contributions during the period of 2017 to 2024 is presented in Table 15.

In addition, a comparison between these control techniques, including advantages and disadvantages has been made. Table 16 summarizes the pros and cons of these control techniques. Each technique has its own advantages and suffers from some limitations. Therefore, each technique is more convenient in specific applications; e.g., scalar control (SC) is adopted in scalar drives for general purpose applications such as pumping and ventilation purposes, while FOC is utilized in servo applications and high-performance AC

drives. DTC is preferred when the industrial process considers the torque as a controlled variable rather than the motor speed. An example of this application is the tension control of wires and paper rolling. Such required operation can be met by using the DTC drive in torque control mode instead of the speed control mode.

Table 15. Research contributions of MPC technique of induction motor drives.

Main Area	Ref.	Core Contribution
MPC	[13]	Examines the application of model predictive control (MPC) in industrial AC drives. Identifies the main obstacles that faces the industrial/commercial acceptance of MPC strategy. Suggests some modifications to enhance performance, aiming to make MPC a competitive alternative to the well-known and commonly used control techniques.
	[241]	Investigating an MPC scheme including flux weakening control for IM drives, applied in EVs. This approach enhances motor operation at high speeds, and system efficiency. By optimizing flux weakening, the torque ripple is reduced, and energy efficiency is enhanced.
	[242]	Presenting a comprehensive review of MPC for electrical drives. The paper outlines fundamental concepts, and improvements in torque control and energy efficiency. The study emphasizes predictive algorithms for multi-objective control.
	[243]	Investigating an optimized MPC scheme for IMs using decision-making algorithms. The method optimizes weighting factors for torque, flux, and switching frequency, enhancing control precision and system efficiency. This approach achieves reduced torque ripples and improved dynamic response.
	[244]	Proposing a robust sensorless MPC system for IM drives. The method enhances torque and flux control precision without relying on speed sensors. Improves dynamic response, reduces torque ripples, and ensures stability under varying operating conditions.
	[245]	Introducing an MPC strategy for six-phase IM drives using Virtual Voltage Vectors (VVVs). This approach enhances torque control, reduces computational complexity, and minimizes torque ripple. It is suitable for multiphase motor drive applications.
	[246]	Proposing a predictive DTC strategy with fault-tolerant functionality for AC motors. The method ensures reliable torque control under fault conditions, enhances system robustness, and maintains operational continuity.
	[247]	Investigating a finite control set predictive DTC scheme for IMs. This approach improves torque and flux control precision and minimizes torque ripple. This method results in high dynamic response and lower switching frequency.
	[248]	Proposing an MPC for IM drives, eliminating weighting factors and current sensors. This approach reduces system complexity and lowers computational burden. It achieves accurate torque and flux control and improved dynamic response.
	[249]	Holding a comparative analysis of MPC for IMs. The study evaluates various approaches, highlighting their impact on torque ripple and dynamic performance.
	[250]	Proposing an MP-Direct Speed control strategy for IM drives. Also compares continuous and finite control set approaches. The method enhances speed control precision, reduces torque ripple, and improves dynamic response.
	[251]	Presenting an optimized predictive control strategy for IM using Artificial Neural Networks (ANNs) to determine cost function parameters. The method achieves adaptive parameter tuning, improved dynamic response, and provides operation at higher efficiency.
	[252]	Proposing an optimized Predictive Torque Control strategy for IMs based on Grey Relational Analysis for objective function optimization. By optimizing the objective function, the method ensures superior dynamic response.
	[253]	Presenting an integrated adaptive sliding mode-based speed control system within FCS-MPC for induction motors. This approach enhances drive robustness and improves torque control. By incorporating adaptive sliding-mode control, better dynamic response is achieved.
	[254]	Proposing a simplified model predictive control (MPC) strategy for AC machines, achieving a high performance with reduced computational complexity. By simplifying the control structure, faster computation and robust performance are achieved.

Table 15. *Cont.*

Main Area	Ref.	Core Contribution
MPC	[255]	Introducing an efficient Predictive Torque Control strategy for IM drives, enhancing torque control precision, reducing torque ripple, and minimizing switching losses. The approach employs an optimized cost function to balance performance and efficiency. This method achieves improved dynamic response and superior energy efficiency.
	[256]	Providing algebraic tuning guidelines for MPC of IM drives. The paper introduces a systematic approach to select control parameters, enhancing torque control precision, flux regulation, and stability. Simplifies controller design suitable for high-performance energy-efficient drives.
	[257]	Holding a comparative study of BLDC motor drive control using finite control set model predictive control (FCS-MPC) and Hysteresis Current Control (HCC). The paper evaluates torque ripples, control precision, and computational complexity. The study ensures the superior dynamic response of FCS-MPC while HCC offers simplicity and ease of implementation. The methodology can be extended to IM drives.

Table 16. A comparison between control techniques of IM drives.

Control Methods	Advantages (Pros)	Disadvantages (Cons)
SC	Satisfactory steady-state performance. Ease of implementation. Applicable with any DAQ systems.	Poor dynamic performance. Not suitable for low-speed applications. Not applicable for servo drives.
FOC	Good transient and steady-state performance. Successful in low-speed applications. Applicable in servo drives.	Online IM parameter identification is needed. A high-speed processing unit is required to implement the control algorithm.
DTC	Quick torque and flux response. Moderate complexity of machine model. Few machine parameters are needed. Sensor-less operation is possible with good accuracy.	The conventional DTC scheme is not applied for servo applications. For low-speed range, stator winding resistance should be estimated to achieve high-performance drive.
MPC	High dynamic performance. Simultaneous optimization of multiple control objectives. Incorporates constraints, ensuring safe operation. Limited torque and current ripples.	High computational complexity. High-speed processing unit is required. Requires accurate motor model. Sensitive to motor parameter variations. Limited industrial acceptance due to high implementation cost.

Regarding the MPC, the industrial adoption is limited due to the requirement of high computational speeds and the processing capability of the digital control unit. Also, MPC needs an accurate model and is sensitive to motor parameter variations.

4.5. Regenerative Braking and Energy Saving

Applying regenerative braking is one of the important strategies that are employed in industrial AC drives and EVs, because it is an effective and efficient energy recovery technique that minimizes the overall energy consumption and provides quick stopping of the electric machine [258–270].

In the case of EVs, this energy is utilized to charge the battery, increasing the distance range of the EV. In medium- and high-power ranges, AC drives apply the regenerative braking technique to return the shaft kinetic energy to the electric grid during braking instants, as in electric trains [14,15].

Research contributions in regenerative braking and energy saving of IM drives during the period 2017 to 2024 are presented and summarized in Table 17.

Table 17. Research contributions in regenerative braking and energy saving of IM drives.

Main Area	Ref.	Core Contribution
Efficiency Optimization	[14]	Investigating energy savings in industrial motor drives. This method enables energy recovery during braking, reduces power loss, and enhances system efficiency. By optimizing bidirectional power flow, the approach achieves higher energy savings, supports regenerative braking, and promotes sustainable, energy-efficient operation in industrial motor drive systems.
	[15]	Proposing a real-time efficiency optimization strategy for IMs. The method dynamically adjusts control parameters to minimize power loss and maximize efficiency during operation. By utilizing an online optimization algorithm, the approach achieves energy savings, supporting energy-efficient and cost-effective motor drive applications.
	[258]	Investigating a Dynamic Energy Distribution (DED) method to enhance energy recovery and utilization efficiency in motor-driven systems. The approach optimally distributes regenerative energy, reducing energy loss and improving system efficiency. By dynamically managing power flow, the method achieves higher energy recovery rates and enhanced operational stability.
	[259]	Introducing an energy saving driving strategy for AC motor driving electric buses. Optimizes speed profiles and driving behaviors to reduce energy consumption. The method incorporates predictive control and real-time traffic data to enhance route efficiency. By minimizing braking and acceleration losses, the approach achieves significant energy savings, extended battery life, and improved operational efficiency.
	[260]	Presenting an optimal energy saving control method for motor drives to extend the range of electric vehicles (EVs). The method optimizes torque and speed control, minimizing energy consumption and enhancing drive efficiency. The scheme ensures an extended driving range.
	[261]	Proposing an optimization strategy to improve the efficiency of electric propulsion systems in electric seaplanes. The method optimizes power distribution, control parameters, and system configuration to reduce energy loss and enhance propulsion efficiency.
	[262]	Introducing an improved energy-efficient starting and operating control technique for single-phase IMs. The method optimizes starting current, reduces energy loss, and enhances motor performance. Achieves smoother starts, lower energy consumption, and improved operational efficiency.
	[263]	Proposing a speed control and efficiency optimization strategy for IMs applied in ventilation fans in mines. The method regulates motor speed to match ventilation demand, reducing energy consumption and operational costs. By optimizing motor efficiency and airflow, the approach ensures considerable energy savings.
	[264]	Investigating an online efficiency optimization and sensorless speed control strategy for single-phase IMs. The method eliminates speed sensors, reducing system complexity and cost. By optimizing motor efficiency in real-time, the approach achieves energy savings and improved dynamic response, thereby supporting energy-efficient IM drives.
	[265]	Introducing an optimal efficiency controller design for pumping systems, aiming to reduce energy consumption and improve operational performance. The method employs advanced control algorithms to optimize motor speed and flow rate, enhancing system efficiency. This approach achieves satisfactory energy savings.
	[266]	Proposing a Hybrid Dragonfly Algorithm to optimize the efficiency of IMs. The method improves energy efficiency by optimizing control parameters, reducing power loss, and improving torque control.
	[267]	Presenting an energy recovery method for four-wheel EVs, relying on braking force distribution. The method optimizes regenerative braking efficiency by balancing braking forces across all wheels. This method improves energy recovery, reduces energy loss, and ensures vehicle stability.
	[268]	Investigating an efficiency optimization control strategy as a regenerative braking system employed in hybrid electric vehicles. The method enhances braking energy recovery, reduces energy loss, and improves system stability.
	[269]	Proposing a regenerative braking strategy for IMs using a pole-changing approach to enhance braking efficiency in EVs. The method improves energy recovery, increases braking torque, and supports variable-speed operation. By changing pole configurations, the approach achieves higher energy recovery.

Table 17. *Cont.*

Main Area	Ref.	Core Contribution
Efficiency Optimization	[270]	Introducing an energy harvesting scheme for harbor cranes using flywheel energy storage systems (FESS). The approach extracts and stores regenerative energy from crane operations, reducing energy waste and grid dependency. The scheme enhances energy efficiency and supports peak load shaving.
	[271]	Presenting an efficiency-optimal MPC strategy for IMs. The method minimizes energy consumption while ensuring precise torque control, thereby improving efficiency under varying load conditions. This scheme achieves an energy-efficient IM motor drive.

5. Manufacturers of Industrial IM Drives

A summary of the well-known industrial AC drive manufacturers (ordered alphabetically) and the employed control techniques in their products are summarized in Table 18. Most manufacturers produce scalar V/F drives and vector control (VC) drives (with position/speed encoder or sensorless drive), while few players adopt DTC technology.

Table 18. Industrial AC drive manufacturers.

Manufacturer	Control Technique			Ref.
	Scalar V/F	VC	DTC	
ABB, Switzerland	Yes	Yes	Yes	[272]
DANFOSS, Denmark	Yes	Yes	No	[273]
DELTA ELECTRONICS, Taiwan	Yes	Yes	No	[274]
EATON, USA	Yes	Yes	No	[275]
EMOTRON, Sweden	Yes	Yes	Yes	[276]
FUJI ELECTRIC, Japan	Yes	Yes	No	[277]
HITACHI, Japan	Yes	Yes	No	[278]
INOMAX, China	Yes	Yes	Yes	[279]
INVERTEK, UK	Yes	Yes	No	[280]
MITSUBISHI, Japan	Yes	Yes	No	[281]
NIDEC, Japan	Yes	Yes	No	[282]
OMRON, Japan	Yes	Yes	No	[283]
ROCKWELL, USA	Yes	Yes	No	[284]
SCHNEIDER, France	Yes	Yes	No	[285]
SIEMENS, Germany	Yes	Yes	Yes	[286]
TOSHIBA, Japan	Yes	Yes	No	[287]
WEG, Brazil	Yes	Yes	No	[288]
YASKAWA, Japan	Yes	Yes	No	[289]

The major observation is that MPC has not yet gained industrial acceptance. However, the PowerFlex® 750 AC drive series, with totalFORCE® technology from Allen-Bradely provides adaptive control of position, velocity, and torque for AC motors [290,291].

6. Modern Applications of IM Drives

Induction motor drives have been employed in many industrial applications for a long time. Recently, they are utilized in modern applications such as:

1. Industrial automation and robotics arms;
2. Electric vehicles, trucks, and buses;

3. High-speed electric trains;
4. Energy saving HVAC systems and inverter-based home air conditions;
5. Drilling rigs in oil and gas industry;
6. Flywheel energy storage systems;
7. Electric propulsion systems in marine applications;
8. Multi-motor conveyor systems;
9. Hoist and crane control to achieve a safe and high-performance operation in terms of anti-sway, including the possibility of regenerative braking to provide quick stopping.

7. Conclusions

Various modern industries depend on induction motor drives, retaining their importance despite the utilization of synchronous motor drives and other types. This article aims to provide a literature summary of the recent trends in high-efficiency induction motor drives during the period of 2017–2024. In addition, the article addresses recent regenerative braking methods and energy saving algorithms incorporated into the induction motor control system. The article is considered as a review guide to junior researchers whose area of interest are AC drives in general, and induction motor drives in specific. Also, the article can help researchers who are interested in power electronics to recognize the recent advancement in WBG-based converters applied in AC motor control. Accordingly, the paper introduces the state-of-the-art publications related to the topic. The novelty of the paper is considered in the topic itself (high-efficiency IM drives), introducing and addressing the recent core contributions related to the topic.

The selected period is narrowed to only the last seven years to include the state-of-the art research activities that have been carried out. However, considerable respectable research publications covering the same topics have been published during the previous two decades, and the pioneer contributions during the last three decades cannot be ignored and have been addressed through the correspondingly covered topics in the article.

The main conclusions and findings are summarized in the following points:

1. Development and adoption of high-efficiency AC drives, especially IM drives, is an important opportunity in the modern industry to reduce energy consumption in different sectors, in accordance with energy efficiency standards and restrictions.
2. Design and implementation of high-efficiency and premium-efficiency IMs have commercial acceptance, as many manufacturers fabricate considerable products covering a wide power range serving multiple applications.
3. Design of high-efficiency IMs using evolutionary optimization techniques and modern analysis tools such as finite element design has received great interest from academia and industry.
4. Many recent research papers are interested in studying and investigating thermal equivalent circuits of IMs to optimize and enhance motor cooling system and increase their efficiency.
5. WBG power semiconductor devices are gradually being incorporated into the development of commercial IM drives due to salient advantages; e.g., SiC devices are suitable for high power applications, while GaN is convenient for low voltage/low power application/very high frequency applications.
6. Some fabrication challenges of WBG power devices still exist; however, considerable research efforts are tackling these obstacles and finding solutions to most of them. Thus, the prices of WBG devices are decreasing with the time to get commercial acceptance.

7. The industrial IM drives still depend on scalar control techniques for general purpose application. Meanwhile, vector control IM drives are used when high-performance drives are required.
8. Until now, few industrial drive manufacturers have adopted or fabricated DTC-based drives since the development of the first drive by ABB in 1996.
9. MPC have not received commercial or industrial acceptance until recently. However, considerable research papers have adopted and recommended the utilization of FCS-MPC in high-performance IM drives.
10. Modern IM drives have the option of regenerative braking to provide quick stopping and motor braking. Moreover, regenerative braking participates in a reduction in the overall energy consumption of AC drives. In EVs and electric transportation systems, regenerative braking extends the distance range of the vehicle battery by trickle charging during EV speed reductions and stopping.

Funding: This research received no external funding.

Conflicts of Interest: The author declares no conflicts of interest.

Abbreviations

ASIC	Application specific integrated circuit
BLDC	Brushless DC motor
CAGR	Compound annual growth rate
CCW	Counterclockwise
CW	Clockwise
DAQ	Data acquisition system
DSP	Digital signal processor
DTC	Direct torque control
ED	Electric drives
EDS	Electric drive system
EMC	Electromagnetic compatibility
EMI	Electromagnetic interference
EV	Electric vehicle
FCS-MPC	Finite control set model predictive control
FO	Field orientation
FOC	Field-oriented control
FPGA	Field programmable gate array
GaN	Gallium nitride
HIL	Hardware in the loop
IM	Induction motor
MPC	Model predictive control
PM	Permanent magnet
PWM	Pulse width modulation
PE	Power electronics
RISC	Reduced instruction set computer
SC	Scalar control
SDGs	Sustainable development goals
SRM	Switched reluctance motor
SVM	Space vector modulation
SiC	Silicon carbide
SRM	Switched reluctance motor
THD	Total harmonic distortion

WBG	Wide bandgap
UN	United nations
VC	Vector control
VSI	Voltage source inverter

Appendix A

Appendix A.1. Sustainable Development Goals of the United Nations

Goal 1: End poverty in all its forms everywhere.

Goal 2: End hunger, achieve food security and improved nutrition, and promote sustainable agriculture.

Goal 3: Ensure healthy lives and promote well-being for all at all ages.

Goal 4: Ensure inclusive and equitable quality education and promote lifelong learning opportunities for all.

Goal 5: Achieve gender equality and empower all women and girls.

Goal 6: Ensure availability and sustainable management of water and sanitation for all.

Goal 7: Ensure access to affordable, reliable, sustainable, and modern energy for all.

Goal 8: Promote sustained, inclusive, and sustainable economic growth, full and productive employment, and decent work for all.

Goal 9: Build resilient infrastructure, promote inclusive and sustainable industrialization, and foster innovation.

Goal 10: Reduce inequality within and among countries.

Goal 11: Make cities and human settlements inclusive, safe, resilient, and sustainable.

Goal 12: Ensure sustainable consumption and production patterns.

Goal 13: Take urgent action to combat climate change and its impacts.

Goal 14: Conserve and sustainably use the oceans, seas, and marine resources for sustainable development.

Goal 15: Protect, restore, and promote sustainable use of terrestrial ecosystems, sustainably manage forests, combat desertification, halt and reverse land degradation, and halt biodiversity loss.

Goal 16: Promote peaceful and inclusive societies for sustainable development, provide access to justice for all, and build effective, accountable, and inclusive institutions at all levels.

Goal 17: Strengthen the means of implementation and revitalize the Global Partnership for Sustainable Development.

Appendix A.2. Summary of Sustainable Development Goals of the United Nations

1. No Poverty.
2. Zero Hunger.
3. Good Health and Well-Being.
4. Quality Education.
5. Gender Equality.
6. Clean Water and Sanitation.
7. Affordable and Clean Energy.
8. Decent Work and Economic Growth.
9. Industry, Innovation and Infrastructure.
10. Reduce Inequality.
11. Sustainable Cities and Communities.
12. Responsible Consumption and Production.
13. Climate Action.

14. Life Below Water.
15. Life on Land.
16. Peace, Justice and Strong Institutions.
17. Partnerships for the Goals

References

1. Electric Drives Market Analysis Report. Available online: https://www.mordorintelligence.com/industry-reports/electric-drives-market (accessed on 15 December 2024).
2. Global AC Drives Industry Research Report. Growth Trends and Competitive Analysis 2022–2028. Available online: https://www.360researchreports.com/global-ac-drives-industry-21727719 (accessed on 15 December 2024).
3. UN-SDGs. Report 2024. Available online: https://unstats.un.org/sdgs/files/report/2024/SG-SDG-Progress-Report-2024-advanced-unedited-version.pdf (accessed on 15 December 2024).
4. UN-SDGs. Report 2023. Available online: https://unstats.un.org/sdgs/report/2023/The-Sustainable-Development-Goals-Report-2023.pdf (accessed on 15 December 2024).
5. Zhao, J.; Xi, X.; Na, Q.; Wang, S.; Kadry, S.N.; Kumar, P.M. The technological innovation of hybrid and plug-in electric vehicles for environment carbon pollution control. *Environ. Impact Assess. Rev.* **2021**, *86*, 106506. [CrossRef]
6. Fuinhas, J.A.; Koengkan, M.; Leitão, N.C.; Nwani, C.; Uzuner, G.; Dehdar, F.; Relva, S.; Peyerl, D. Effect of Battery Electric Vehicles on Greenhouse Gas Emissions in 29 European Union Countries. *Sustainability* **2021**, *13*, 13611. [CrossRef]
7. Azab, M. Low-Cost DTC Drive Using Four-Switch Inverter for Low Power Ranges. *Vehicles* **2024**, *6*, 895–919. [CrossRef]
8. Parv, A.L.; Daicu, R.; Dragoi, M.V.; Rusu, M.; Oancea, G. A Method to Design Assembling Lines for Super Premium Efficiency Motors. *Processes* **2023**, *11*, 215. [CrossRef]
9. Dems, M.; Komeza, K. Designing an Energy-Saving Induction Motor Operating in a Wide Frequency Range. *IEEE Trans. Ind. Electron.* **2022**, *69*, 4387–4397. [CrossRef]
10. Chen, Z.; Huang, A.Q. Extreme high efficiency enabled by silicon carbide (SiC) power devices. *Mater. Sci. Semicond. Process.* **2024**, *172*, 108052. [CrossRef]
11. Xu, Y.; Yuan, X.; Ye, F.; Wang, Z.; Zhang, Y.; Diab, M.; Zhou, W. Impact of High Switching Speed and High Switching Frequency of Wide-Bandgap Motor Drives on Electric Machines. *IEEE Access* **2021**, *9*, 82866–82880. [CrossRef]
12. Takahashi, I.; Noguchi, T. A new quick-response and high-efficiency control strategy of an induction motor. *IEEE Trans. Indus. App.* **1986**, *22*, 820–827. [CrossRef]
13. Mirzaeva, G.; Mo, Y. Model Predictive Control for Industrial Drive Applications. *IEEE Trans. Ind. Appl.* **2023**, *59*, 7897–7907. [CrossRef]
14. Karatzaferis, I.; Tatakis, E.C.; Papanikolaou, N. Investigation of Energy Savings on Industrial Motor Drives Using Bidirectional Converters. *IEEE Access* **2017**, *5*, 17952–17961. [CrossRef]
15. Farhani, F.; Zaafouri, A.; Chaari, A. Real time induction motor efficiency optimization. *J. Frankl. Inst.* **2017**, *354*, 3289–3304. [CrossRef]
16. Available online: https://www.ti.com/lit/pdf/sprabq0 (accessed on 15 December 2024).
17. Available online: https://www.typhoon-hil.com/solutions/power-electronics/electric-motor-drives/ (accessed on 15 December 2024).
18. Wu, Z.; Xie, B.; Li, Z.; Mitsuoka, M.; Inoue, E.; Okayasu, T.; Hirai, Y. DSPACE based Hardware in the loop Testing Platform for Powertrain Management Unit of Electric Tractor. *J. Fac. Agric. Kyushu Univ.* **2019**, *64*, 309–317. [CrossRef]
19. Kim, H.-J.; Lee, C.-S. Shape Parameters Design for Improving Energy Efficiency of IPM Traction Motor for EV. *IEEE Trans. Veh. Technol.* **2021**, *70*, 6662–6673. [CrossRef]
20. Lu, S.-M. A review of high-efficiency motors: Specification, policy, and technology. *Renew. Sustain. Energy Rev.* **2016**, *59*, 1–12. [CrossRef]
21. Nardo, M.D.; Marfoli, A.; Degano, M.; Gerada, C. Rotor Slot Design of Squirrel Cage Induction Motors with Improved Rated Efficiency and Starting Capability. *IEEE Trans. Ind. Appl.* **2022**, *58*, 3383–3393. [CrossRef]
22. Marfoli, A.; Nardo, M.D.; Degano, M.; Gerada, C.; Chen, W. Rotor Design Optimization of Squirrel Cage Induction Motor-Part I: Problem Statement. *IEEE Trans. Energy Convers.* **2021**, *36*, 1271–1279. [CrossRef]
23. Zhang, J.; Cui, R.; Wei, Y.; Yu, D.; Xie, S.; Fang, S.; Shen, J. Optimization and Experimental Validation of Amorphous Alloy High-Speed Asynchronous Motor for Simultaneous Reduction on Core and Copper Losses. *IEEE Access* **2023**, *11*, 101112–101122. [CrossRef]
24. Popescu, M.; Di Leonardo, L.; Fabri, G.; Volpe, G.; Riviere, N.; Villani, M. Design of Induction Motors with Flat Wires and Copper Rotor for E-Vehicles Traction System. *IEEE Trans. Ind. Appl.* **2023**, *59*, 3889–3900. [CrossRef]

25. Mei, J.; Lee, C.H.T.; Kirtley, J.L. Design of Axial Flux Induction Motor with Reduced Back Iron for Electric Vehicles. *IEEE Trans. Veh. Technol.* **2020**, *69*, 293–301. [CrossRef]
26. Tran, T.-V.; Nègre, E.; Mikati, K.; Pellerey, P.; Assaad, B. Optimal Design of TEFC Induction Machine and Experimental Prototype Testing for City Battery Electric Vehicle. *IEEE Trans. Ind. Appl.* **2020**, *56*, 635–643. [CrossRef]
27. Ion, C.P.; Peter, I. Manufacturing of induction motors with Super Premium Efficiency. In Proceedings of the 2022 International Conference and Exposition on Electrical and Power Engineering (EPE), Iasi, Romania, 20–22 October 2022; pp. 47–50. [CrossRef]
28. Kim, M.-S.; Park, J.-H.; Lee, K.-S.; Lee, S.-H.; Choi, J.-Y. Performance Characteristics of the Rotor Conductor of an IE4 Class Induction Motor with Varying Al-Cu Ratio. *IEEE Trans. Magn.* **2022**, *58*, 1–6. [CrossRef]
29. Gundogdu, T.; Suli, S. Role of End-Ring Configuration in Shaping IE4 Induction Motor Performance. *CES Trans. Electr. Mach. Syst.* **2024**, *8*, 245–254. [CrossRef]
30. Aishwarya, M.; Brisilla, R.M. Design of Energy-Efficient Induction motor using ANSYS software. *Results Eng.* **2022**, *16*, 100616. [CrossRef]
31. Alberti, L.; Troncon, D. Design of Electric Motors and Power Drive Systems According to Efficiency Standards. *IEEE Trans. Ind. Electron.* **2021**, *68*, 9287–9296. [CrossRef]
32. Marfoli, A.; DiNardo, M.; Degano, M.; Gerada, C.; Jara, W. Squirrel Cage Induction Motor: A Design-Based Comparison between Aluminium and Copper Cages. *IEEE Open J. Ind. Appl.* **2021**, *2*, 110–120. [CrossRef]
33. Cavagnino, A.; Vaschetto, S.; Ferraris, L.; Gmyrek, Z.; Agamloh, E.B.; Bramerdorfer, G. Striving for the Highest Efficiency Class with Minimal Impact for Induction Motor Manufacturers. *IEEE Trans. Ind. Appl.* **2020**, *56*, 194–204. [CrossRef]
34. Usha, S.; Subramani, C.; Raman, A.; Bhaduri, M.; Doss, M.A.N.; Puri, R. Efficiency Improvement of Induction Motor Through Altered Design. *Int. J. Recent Technol. Eng.* **2019**, *8*, 3429–3435.
35. Khan, K.; Shukla, S.; Sing, B. Design and Development of High Efficiency Induction Motor for PV Array Fed Water Pumping. In Proceedings of the 2018 IEEE International Conference on Power Electronics, Drives and Energy Systems (PEDES), Chennai, India, 18–21 December 2018; pp. 1–6. [CrossRef]
36. Tig, I.; Imeryuz, M.; Akcomak, M.; Polat, A. Design of High Efficient 1.1 kW 8 Pole Induction Motor for Industrial Application. In Proceedings of the 2023 14th International Conference on Electrical and Electronics Engineering (ELECO), Bursa, Türkiye, 30 November–2 December 2023; pp. 1–5. [CrossRef]
37. Asgharpour-Alamdari, H.; Alinejad-Beromi, Y.; Yaghobi, H. Improvement of induction motor operation using a new winding scheme for reduction of the magnetomotive force distortion. *IET Electr. Power Appl.* **2018**, *12*, 323–331. [CrossRef]
38. Kim, H.M.; Lee, K.W.; Kim, D.G.; Park, J.H.; Park, G.S. Design of Cryogenic Induction Motor Submerged in Liquefied Natural Gas. *IEEE Trans. Magn.* **2018**, *54*, 1–4. [CrossRef]
39. Verucchi, C.; Ruschetti, C.; Giraldo, E.; Bossio, G.; Bossio, J. Efficiency optimization in small induction motors using magnetic slot wedges. *Electr. Power Syst. Res.* **2017**, *152*, 1–8. [CrossRef]
40. Shao, L.; Karci, A.E.H.; Tavernini, D.; Sorniotti, A.; Cheng, M. Design Approaches and Control Strategies for Energy-Efficient Electric Machines for Electric Vehicles—A Review. *IEEE Access* **2020**, *8*, 116900–116913. [CrossRef]
41. Dems, M.; Komeza, K.; Szulakowski, J.; Kubiak, W. Increase the Efficiency of an Induction Motor Feed from Inverter for Low Frequencies by Combining Design and Control Improvements. *Energies* **2022**, *15*, 530. [CrossRef]
42. Sharma, U.; Singh, B. Design and Development of Energy Efficient Single Phase Induction Motor for Ceiling Fan Using Taguchi's Orthogonal Arrays. *IEEE Trans. Ind. Appl.* **2021**, *57*, 3562–3572. [CrossRef]
43. Zhao, N.; Schofield, N. An Induction Machine Design with Parameter Optimization for a 120-kW Electric Vehicle. *IEEE Trans. Transp. Electrif.* **2020**, *6*, 592–601. [CrossRef]
44. Silva, A.M.; Ferreira, F.J.T.E.; Cistelecan, M.V.; Antunes, C.H. Multiobjective Design Optimization of Generalized Multilayer Multiphase AC Winding. *IEEE Trans. Energy Convers.* **2019**, *34*, 2158–2167. [CrossRef]
45. Aishwarya, M.; Brisilla, R.M. Design and Fault Diagnosis of Induction Motor Using ML-Based Algorithms for EV Application. *IEEE Access* **2023**, *11*, 34186–34197. [CrossRef]
46. Xu, W.; Xiao, X.; Du, G.; Hu, D.; Zou, J. Comprehensive Efficiency Optimization of Linear Induction Motors for Urban Transit. *IEEE Trans. Veh. Technol.* **2020**, *69*, 131–139. [CrossRef]
47. Mahmouditabar, F.; Baker, N.J. Design Optimization of Induction Motors with Different Stator Slot Rotor Bar Combinations Considering Drive Cycle. *Energies* **2023**, *17*, 154. [CrossRef]
48. Lei, A.; Song, C.-X.; Lei, Y.-L.; Fu, Y. Design optimization of vehicle asynchronous motors based on fractional harmonic response analysis. *Mech. Sci.* **2021**, *12*, 689–700. [CrossRef]
49. Bortoni, E.C.; Bernardes, J.V.; da Silva, P.V.; Faria, V.A.; Vieira, P.A. Evaluation of manufacturers strategies to obtain high-efficient induction motors. *Sustain. Energy Technol. Assess.* **2019**, *31*, 221–227. [CrossRef]
50. Kabir, M.A.; Jaffar, M.Z.M.; Wan, Z.; Husain, I. Design, Optimization, and Experimental Evaluation of Multilayer AC Winding for Induction Machine. *IEEE Trans. Ind. Appl.* **2019**, *55*, 3630–3639. [CrossRef]

51. Bianchini, C.; Vogni, M.; Torreggiani, A.; Nuzzo, S.; Barater, D.; Franceschini, G. Slot Design Optimization for Copper Losses Reduction in Electric Machines for High Speed Applications. *Appl. Sci.* **2020**, *10*, 7425. [CrossRef]
52. Akhtar, M.J.; Behera, R.K. Optimal design of stator and rotor slot of induction motor for electric vehicle applications. *IET Electr. Syst. Transp.* **2019**, *9*, 35–43. [CrossRef]
53. Mallik, S.; Mallik, K.; Barman, A.; Maiti, D.; Biswas, S.K.; Deb, N.K.; Basu, S. Efficiency and Cost Optimized Design of an Induction Motor Using Genetic Algorithm. *IEEE Trans. Ind. Electron.* **2017**, *64*, 9854–9863. [CrossRef]
54. Kim, M.-S.; Kim, C.-E. Multi-Objective Optimum Design of Premium High Efficiency Induction Motor Using Parameter Learning. *Trans. Korean Inst. Electr. Eng. KIEE* **2021**, *70*, 991–998. [CrossRef]
55. Laouar, I.; Boukadoum, A. Design Optimization of a Three-Phase Squirrel-Cage Induction Motor by Algorithm Harmony Search. In Proceedings of the 2022 IEEE International Conference on Electrical Sciences and Technologies in Maghreb (CISTEM), Tunis, Tunisia, 26–28 October 2022; pp. 1–6. [CrossRef]
56. Srimathi, R.; Ponmurugan, P.; Iqbal, A.; Kamatchi, K.V.; Lakshmanan, M.; Nadin, E.S. A More Efficient Induction Machine based on Hill Climbing Local Search Optimization. In Proceedings of the 2022 International Virtual Conference on Power Engineering Computing and Control: Developments in Electric Vehicles and Energy Sector for Sustainable Future (PECCON), Chennai, India, 5–6 May 2022; pp. 1–6. [CrossRef]
57. Bian, Y.; Yang, Z.; Sun, X.; Wang, X. Speed Sensorless Control of a Bearingless Induction Motor Based on Modified Robust Kalman Filter. *J. Electr. Eng. Technol.* **2024**, *19*, 1179–1190. [CrossRef]
58. Su, Y.; Yang, Z.; Sun, X.; Shen, Z. Direct torque control of bearingless induction motor based on super-twisting sliding mode control. *J. Control. Decis.* **2024**, 1–11. [CrossRef]
59. Ye, X.; Tang, X.; Xing, K.; Wang, H.; Yao, J.; Zhang, T. Repetitive Control for Vibration Suppression of Bearingless Induction Motor. *IEEE Access* **2024**, *12*, 60532–60540. [CrossRef]
60. Su, Y.; Yang, Z.; Sun, X.; Ding, Q. Backstepping control of a bearingless induction motor based on a linear extended state observer. *Electr Eng* **2023**, *105*, 4569–4579. [CrossRef]
61. Yang, Z.; Jia, J.; Sun, X.; Xu, T. A Fuzzy-ELADRC Method for a Bearingless Induction Motor. *IEEE Trans. Power Electron.* **2022**, *37*, 11803–11813. [CrossRef]
62. Chen, J.; Fujii, Y.; Johnson, M.W.; Farhan, A.; Severson, E.L. Optimal Design of the Bearingless Induction Motor. *IEEE Trans. Ind. Appl.* **2021**, *57*, 1375–1388. [CrossRef]
63. Chen, J.; Severson, E.L. Design and Modeling of the Bearingless Induction Motor. In Proceedings of the 2019 IEEE International Electric Machines & Drives Conference (IEMDC), San Diego, CA, USA, 12–15 May 2019; pp. 343–350. [CrossRef]
64. Sinervo, A.; Arkkio, A. Rotor Radial Position Control and its Effect on the Total Efficiency of a Bearingless Induction Motor with a Cage Rotor. *IEEE Trans. Magn.* **2014**, *50*, 1–9. [CrossRef]
65. Chen, J.; Zhu, J.; Severson, E.L. Review of Bearingless Motor Technology for Significant Power Applications. *IEEE Trans. Ind. Appl.* **2020**, *56*, 1377–1388. [CrossRef]
66. Severson, E.L.; Nilssen, R.; Undeland, T.; Mohan, N. Design of Dual Purpose No-Voltage Combined Windings for Bearingless Motors. *IEEE Trans. Ind. Appl.* **2017**, *53*, 4368–4379. [CrossRef]
67. Chen, J.; Johnson, M.W.; Farhan, A.; Wang, Z.; Fujii, Y.; Severson, E.L. Reduced Axial Length Pole-Specific Rotor for Bearingless Induction Machines. *IEEE Trans. Energy Convers.* **2022**, *37*, 2285–2297. [CrossRef]
68. Yang, Z.; Ding, Q.; Sun, X.; Lu, C. Design and Analysis of a Three-Speed Wound Bearingless Induction Motor. *IEEE Trans. Ind. Electron.* **2022**, *69*, 12529–12539. [CrossRef]
69. Fang, W.; Yang, Z.; Sun, X.; Wang, G.; Xu, T. Speed Sensorless Control of Bearingless Induction Motors Based on Adaptive Flux Observer. *J. Electr. Eng. Technol.* **2022**, *17*, 1803–1813. [CrossRef]
70. Carvalho Souza, F.E.; Silva, W.; Ortiz Salazar, A.; Paiva, J.; Moura, D.; Villarreal, E.R.L. A Novel Driving Scheme for Three-Phase Bearingless Induction Machine with Split Winding. *Energies* **2021**, *14*, 4930. [CrossRef]
71. Ye, X.; Yang, Z. Development of bearingless induction motors and key technologies. *IEEE Access* **2019**, *7*, 121055–121066. [CrossRef]
72. Lu, J.; Yang, Z.; Sun, X.; Bao, C.; Chen, X. Direct Levitation Force Control for a Bearingless Induction Motor Based on Model Prediction. *IEEE Access* **2019**, *7*, 65368–65378. [CrossRef]
73. Chen, J.; Severson, E.L. Optimal Design of the Bearingless Induction Motor for Industrial Applications. In Proceedings of the 2019 IEEE Energy Conversion Congress and Exposition (ECCE), Baltimore, MD, USA, 29 September–3 October 2019; pp. 5265–5272. [CrossRef]
74. Nunes, E.A.D.F.; Salazar, A.O.; Villarreal, E.R.L.; Souza, F.E.C.; Dos Santos Júnior, L.P.; Lopes, J.S.B.; Luque, J.C.C. Proposal of a fuzzy controller for radial position in a bearingless induction motor. *IEEE Access* **2019**, *7*, 114808–114816. [CrossRef]
75. Asama, J.; Oi, T.; Oiwa, T.; Chiba, A. Simple Driving Method for a 2-DOF Controlled Bearingless Motor Using One Three-Phase Inverter. *IEEE Trans. Ind. Appl.* **2018**, *54*, 4365–4376. [CrossRef]

76. Yang, Z.; Chen, L.; Sun, X.; Sun, W.; Zhang, D. A Bearingless Induction Motor Direct Torque Control and Suspension Force Control Based on Sliding Mode Variable Structure. *Math. Probl. Eng.* **2017**, *2409179*, 11. [CrossRef]
77. Han, P.-W.; Seo, U.-J.; Paul, S.; Chang, J. Computationally Efficient Stator AC Winding Loss Analysis Model for Traction Motors Used in High-Speed Railway Electric Multiple Unit. *IEEE Access* **2022**, *10*, 28725–28738. [CrossRef]
78. Tabora, J.M.; Tostes, M.E.D.L.; Bezerra, U.H.; De Matos, E.O.; Filho, C.L.P.; Soares, T.M.; Rodrigues, C.E.M. Assessing Energy Efficiency and Power Quality Impacts Due to High-Efficiency Motors Operating Under Nonideal Energy Supply. *IEEE Access* **2021**, *9*, 121871–121882. [CrossRef]
79. Gómez, J.R.; Sousa, V.; Eras, J.J.C.; Gutiérrez, A.S.; Viego, P.R.; Quispe, E.C.; de León, G. Assessment criteria of the feasibility of replacement standard efficiency electric motors with high-efficiency motors. *Energy* **2022**, *239*, 121877. [CrossRef]
80. Yang, Z.; Sun, C.; Sun, X.; Sun, Y. An improved dynamic model for bearingless induction motor considering rotor eccentricity and load change. *IEEE Trans. Ind. Electron.* **2021**, *69*, 3439–3448. [CrossRef]
81. Mei, J.; Zuo, Y.; Lee, C.H.T.; Kirtley, J.L. Modeling and Optimizing Method for Axial Flux Induction Motor of Electric Vehicles. *IEEE Trans. Veh. Technol.* **2020**, *69*, 12822–12831. [CrossRef]
82. Ali, M.Z.; Shabbir, M.N.S.K.; Liang, X.; Zhang, Y.; Hu, T. Machine learning-based fault diagnosis for single- and multi-faults in induction motors using measured stator currents and vibration signals. *IEEE Trans. Ind. Appl.* **2019**, *55*, 2378–2391. [CrossRef]
83. Wang, K.; Huai, R.; Yu, Z.; Zhang, X.; Li, F.; Zhang, L. Comparison Study of Induction Motor Models Considering Iron Loss for Electric Drives. *Energies* **2019**, *12*, 503. [CrossRef]
84. Liu, Y.; Bazzi, A.M. A General Analytical Three-Phase Induction Machine Core Loss Model in the Arbitrary Reference Frame. *IEEE Trans. Ind. Appl.* **2017**, *53*, 4210–4220. [CrossRef]
85. Konda, Y.R.; Ponnaganti, V.K.; Reddy, P.V.S.; Singh, R.R.; Mercorelli, P.; Gundabattini, E.; Solomon, D.G. Thermal Analysis and Cooling Strategies of High-Efficiency Three-Phase Squirrel-Cage Induction Motors—A Review. *Computation* **2024**, *12*, 6. [CrossRef]
86. Madhavan, S.; P B, R.D.; Gundabattini, E.; Mystkowski, A. Thermal Analysis and Heat Management Strategies for an Induction Motor, a Review. *Energies* **2022**, *15*, 8127. [CrossRef]
87. Assaad, B.; Mikati, K.; Tran, T.V.; Negre, E. Experimental Study of Oil Cooled Induction Motor for Hybrid and Electric Vehicles. In Proceedings of the 2018 XIII International Conference on Electrical Machines (ICEM), Alexandroupoli, Greece, 3–6 September 2018; pp. 1195–1200. [CrossRef]
88. Gundabattini, E.; Kuppan, R.; Solomon, D.G.; Kalam, A.; Kothari, D.; Abu Bakar, R. A review on methods of finding losses and cooling methods to increase the efficiency of electric machines. *Ain Shams Eng. J.* **2021**, *12*, 497–505. [CrossRef]
89. Cabral, P.; Adouni, A. Induction Motor Thermal Analysis Based on Lumped Parameter Thermal Network. *KnE Eng.* **2020**, *5*, 451–464. [CrossRef]
90. Zhong, S.; Tschida, C.; Bednarowski, D. Thermal Analysis of Water-Cooled Totally Enclosed Non-Ventilated Induction Motor. In Proceedings of the SoutheastCon 2024, Atlanta, GA, USA, 15–24 March 2024; pp. 793–798. [CrossRef]
91. Madhavan, S.; P B, R.D.; Konda, Y.R.; Gundabattini, E.; Mystkowski, A.; Palka, R.; Wardach, M.; Prajzendanc, P. Thermal management analyses of induction motor through the combination of air-cooling and an integrated water-cooling system. *Sci. Rep.* **2023**, *13*, 10125. [CrossRef]
92. Bucho, L.F.D.; Fernandes, J.F.P.; Biasion, M.; Vaschetto, S.; Cavagnino, A. Experimental Assessment of Cryogenic Cooling Impact on Induction Motors. *IEEE Trans. Energy Convers.* **2022**, *37*, 2629–2636. [CrossRef]
93. Deriszadeh, A.; de Monte, F. On heat transfer performance of cooling systems using nanofluid for electric motor applications. *Entropy* **2020**, *22*, 99. [CrossRef]
94. Abdullah, A.T.; Ali, A.M. Thermal analysis of a three-phase induction motor based on motor-CAD, flux2D, and Matlab. *Indones. J. Electr. Eng. Comput. Sci.* **2019**, *15*, 48–55. [CrossRef]
95. Adouni, A.; Marques Cardoso, A.J. Thermal analysis of low-power three-phase induction motors operating under voltage unbalance and inter-turn short circuit faults. *Machines* **2020**, *9*, 2. [CrossRef]
96. Appadurai, M.; Raj, E.F.I.; Venkadeshwaran, K. Finite element design and thermal analysis of an induction motor used for a hydraulic pumping system. *Mater. Today Proc.* **2021**, *45*, 7100–7106. [CrossRef]
97. Putra, N.; Ariantara, B. Electric motor thermal management system using L-shaped flat heat pipes. *Appl. Therm. Eng.* **2017**, *126*, 1156–1163. [CrossRef]
98. Ahmed, F.; Kar, N.C. Analysis of End-Winding Thermal Effects in an Enclosed Fan-Cooled Induction Motor with a Die-Cast Copper Rotor. *IEEE Trans. Ind. Appl.* **2017**, *53*, 3098–3109. [CrossRef]
99. Towhidi, M.; Ahmed, F.; Mollaeian, A.; Kar, N.C. Thermal Modelling of an Induction Motor with Liquid Cooling Optimization for Different EV Drive Cycles. In Proceedings of the 2020 10th International Electric Drives Production Conference (EDPC), Ludwigsburg, Germany, 8–9 December 2020; pp. 1–6. [CrossRef]

100. Kim, M.-S.; Park, J.-H.; Lee, K.-S.; Lee, S.-H.; Choi, J.-Y. Optimum Design of Cooling Fan considering Experimental Method for Three-Phase Induction Motor. In Proceedings of the 2020 23rd International Conference on Electrical Machines and Systems (ICEMS), Hamamatsu, Japan, 24–27 November 2020; pp. 1220–1224. [CrossRef]
101. Boglietti, A.; Nategh, S.; Carpaneto, E.; Boscaglia, L.; Scema, C. An optimization method for cooling system design of traction motors. In Proceedings of the 2019 IEEE International Electric Machines and Drives Conference (IEMDC), San Diego, CA, USA, 12–15 May 2019; pp. 1210–1215.
102. Satrústegui, M.; Martinez-Iturralde, M.; Ramos, J.C.; Gonzalez, P.; Astarbe, G.; Elosegui, I. Design criteria for water cooled systems of induction machines. *Appl. Therm. Eng.* **2017**, *5*, 1018–1028. [CrossRef]
103. Available online: https://library.e.abb.com/public/e35d57ce4df3160285257d6d00720f51/9AKK106369_SuperE_1014_WEB.pdf (accessed on 15 December 2024).
104. Available online: https://www.lafertaust.com.au/wp-content/uploads/2019/02/Lafert-Catalogue-AC-motors-2018.pdf (accessed on 15 December 2024).
105. Available online: https://static.weg.net/medias/downloadcenter/hae/hdc/US100-Standard-Catalog-Super-Premium-and-Explosion-Proof-Sections.pdf (accessed on 15 December 2024).
106. Available online: https://www.leadgomotor.com/ye3%EF%BC%88ie3%EF%BC%89series-premium-efficiency-three-phase-asynchronous-motor/ (accessed on 15 December 2024).
107. Available online: https://apsrewinds.com.au/wp-content/uploads/specs_attach/Catalogue%20Toshiba%20LVM%20Premium%20Efficiency%20A4%201209.pdf (accessed on 15 December 2024).
108. Ning, P.; Hui, X.; Li, D.; Kang, Y.; Yang, J.; Liu, C. Review of Thermal Design of SiC Power Module for Motor Drive in Electrical Vehicle Application. *CES Trans. Electr. Mach. Syst.* **2024**, *8*, 332–346. [CrossRef]
109. Liu, C.; Zhuang, K.; Pei, Z.; Zhu, D.; Li, X.; Yu, Q.; Xin, H. Hybrid SiC-Si DC–AC Topology: SHEPWM Si-IGBT Master Unit Handling High Power Integrated with Partial-Power SiC-MOSFET Slave Unit Improving Performance. *IEEE Trans. Power Electron.* **2022**, *37*, 3085–3098. [CrossRef]
110. Baek, S.; Cho, Y.; Cho, B.-G.; Hong, C. Performance Comparison Between Two-Level and Three-Level SiC-Based VFD Applications with Output Filters. *IEEE Trans. Ind. Appl.* **2019**, *55*, 4770–4779. [CrossRef]
111. Morya, A.K.; Gardner, M.C.; Anvari, B.; Liu, L.; Yepes, A.G.; Doval-Gandoy, J.; Toliyat, H.A. Wide Bandgap Devices in AC Electric Drives: Opportunities and Challenges. *IEEE Trans. Transp. Electrif.* **2019**, *5*, 3–20. [CrossRef]
112. Schroedermeier, A.; Ludois, D.C. Integration of Inductors, Capacitors, and Damping Into Bus Bars for Silicon Carbide Inverter dv/dt Filters. *IEEE Trans. Ind. Appl.* **2019**, *55*, 5045–5054. [CrossRef]
113. Loncarski, J.; Monopoli, V.G.; Leuzzi, R.; Ristic, L.; Cupertino, F. Analytical and Simulation Fair Comparison of Three Level Si IGBT Based NPC Topologies and Two Level SiC MOSFET Based Topology for High Speed Drives. *Energies* **2019**, *12*, 4571. [CrossRef]
114. Taniguchi, H.; Kondo, K.; Koiwa, K.; Natori, K.; Fujimoto, K.; Makishima, S. Analysis of Energy-Saving Effect for Applying a SiC Switching Device to Inverters for Railway Vehicles Drives. *IEEJ J. Ind. Appl.* **2024**, *13*, 105–112. [CrossRef]
115. Cittanti, D.; Vico, E.; Bojoi, I.R. New FOM-Based Performance Evaluation of 600/650 V SiC and GaN Semiconductors for Next-Generation EV Drives. *IEEE Access* **2022**, *10*, 51693–51707. [CrossRef]
116. Fard, M.T.; Abarzadeh, M.; Noghani, K.A.; He, J.; Al-Haddad, K. Si/SiC hybrid 5-level active NPC inverter for electric aircraft propulsion drive applications. *Chin. J. Electr. Eng.* **2020**, *6*, 63–76. [CrossRef]
117. Fujishima, N. Technical Trends of SiC Power Semiconductor Devices and Their Applications in Power Electronics. *IEEJ J. Ind. Appl.* **2024**, *13*, 372–378. [CrossRef]
118. Yao, W.; Lu, J.; Taghizadeh, F.; Bai, F.; Seagar, A. Integration of SiC Devices and High-Frequency Transformer for High-Power Renewable Energy Applications. *Energies* **2023**, *16*, 1538. [CrossRef]
119. Li, Q.; Zhang, X.; Yuan, C.; Ma, J.; Jiang, D. Variable Switching Frequency DPWM for ZVS in AC Motor Drive Fed by Two Paralleled SiC Inverters with Coupled Inductors. *IEEE Trans. Power Electron.* **2024**, *39*, 1308–1318. [CrossRef]
120. Horowitz, K.; Reese, S.; Remo, T. Research Highlight. In *Manufacturing: SiC Power Electronics for Variable Frequency Motor Drives. Research Highlight in Manufaturing Analysis*; NREL/BR-6A20-68103; National Renewable Energy Laboratory: Applewood, CO, USA, 2017. Available online: https://www.nrel.gov/docs/fy17osti/68103.pdf (accessed on 15 December 2024).
121. Zhou, W.; Diab, M.; Yuan, X.; Wei, C. Mitigation of Motor Overvoltage in SiC-Based Drives Using Soft-Switching Voltage Slew-Rate (dv/dt) Profiling. *IEEE Trans. Power Electron.* **2022**, *37*, 9612–9628. [CrossRef]
122. Sundeep, S.; Wang, J.; Griffo, A.; Alvarez-Gonzalez, F. Antiresonance Phenomenon and Peak Voltage Stress Within PWM Inverter Fed Stator Winding. *IEEE Trans. Ind. Electron.* **2021**, *68*, 11826–11836. [CrossRef]
123. Li, Y.; Zhang, Y.; Yuan, X.; Zhang, L.; Song, Z.; Wu, M.; Ye, F.; Li, Z.; Li, Y.; Xu, Y.; et al. 500 kW Forced Air-Cooled Silicon Carbide (SiC) Three-Phase DC/AC Converter with a Power Density of 1.246 MW/m^3 and Efficiency >98.5%. *IEEE Trans. Ind. Appl.* **2021**, *57*, 5013–5027. [CrossRef]

124. Kawamura, A.; Tsuruta, Y.; Obara, H. Over 99.7% Efficiency at 100 kW DC-DC Power Conversion using a 3.3 kV SiC Device and Discussion on Device *dv/dt* Estimation. *IEEJ J. Ind. Applications* **2024**, *13*, 426–436. [CrossRef]
125. Woldegiorgis, D.; Hossain, M.M.; Saadatizadeh, Z.; Wei, Y.; Mantooth, H.A. Hybrid Si/SiC Switches: A Review of Control Objectives, Gate Driving Approaches and Packaging Solutions. *IEEE J. Emerg. Sel. Top. Power Electron.* **2023**, *11*, 1737–1753. [CrossRef]
126. Baliga, B.J. Silicon Carbide Power Devices: Progress and Future Outlook. *IEEE J. Emerg. Sel. Top. Power Electron.* **2023**, *11*, 2400–2411. [CrossRef]
127. Zhang, B.Y.; Wang, S.; Lai, Y.; Yang, Y. Modeling and Prediction of Low-frequency Radiated EMI for a SiC Motor Drive System. *IEEE Trans. Ind. Electron.* **2023**, *71*, 10210–10220. [CrossRef]
128. DeBoi, B.T.; Lemmon, A.N.; McPherson, B.; Passmore, B. Improved Methodology for Parasitic Analysis of High-Performance Silicon Carbide Power Modules. *IEEE Trans. Power Electron.* **2022**, *37*, 12415–12425. [CrossRef]
129. Zhang, L.; Yuan, X.; Wu, X.; Shi, C.; Zhang, J.; Zhang, Y. Performance Evaluation of High-Power SiC MOSFET Modules in Comparison to Si IGBT Modules. *IEEE Trans. Power Electron.* **2019**, *34*, 1181–1196. [CrossRef]
130. Li, X.; Jiang, J.; Huang, A.Q.; Guo, S.; Deng, X.; Zhang, B.; She, X. A SiC Power MOSFET Loss Model Suitable for High-Frequency Applications. *IEEE Trans. Ind. Electron.* **2017**, *64*, 8268–8276. [CrossRef]
131. Stefanik, J.; Zygmanowski, M. Power Loss Analysis of Advanced-Neutral-Point-Clamped Converter with SiC MOSFETs and Si IGBTs. In Proceedings of the 2021 IEEE 19th International Power Electronics and Motion Control Conference (PEMC), Gliwice, Poland, 25–29 April 2021; pp. 161–166.
132. Abdelrahman, A.; Erdem, Z.; Attia, Y.; Youssef, M. Performance of Wide Band Gap Devices in Electric Vehicles Converters: A Case Study Evaluation. In Proceedings of the 2018 20th European Conference on Power Electronics and Applications (EPE'18 ECCE Europe), Riga, Latvia, 17–21 September 2018; pp. 1–9.
133. Yu, S.; Wang, J.; Zhang, X.; Liu, Y.; Jiang, N.; Wang, W. The potential impact of using traction inverters with SiC MOSFETs for electric buses. *IEEE Access* **2021**, *9*, 51561–51572. [CrossRef]
134. Nisch, A.; Heller, M.; Wondrak, W.; Bucher, A.; Hasenohr, C.; Kefer, K.; Lunz, B.; Pawellek, A.; Smit, A.; Gärtner, M.; et al. Simulation and Measurement-Based Analysis of Efficiency Improvement of SiC MOSFETs in a Series-Production Ready 300 KW/400 V Automotive Traction Inverter. In Proceedings of the 2020 22nd European Conference on Power Electronics and Applications (EPE'20 ECCE Europe), Lyon, France, 7–11 September 2020; pp. 1–10.
135. Ding, X.; Du, M.; Duan, C.; Guo, H.; Xiong, R.; Xu, J.; Cheng, J.; Luk, P.C.K. Analytical and Experimental Evaluation of SiC-Inverter Nonlinearities for Traction Drives Used in Electric Vehicles. *IEEE Trans. Veh. Technol.* **2018**, *67*, 146–159. [CrossRef]
136. Halder, S.; Bhuvir, K.; Bhattacharjee, S.; Nakka, J.; Panda, A.; Ghosh, M. Performance Analysis of WBG Inverter Fed Electric Traction Drive System for EV Application. In Proceedings of the 2023 IEEE IAS Global Conference on Renewable Energy and Hydrogen Technologies (GlobConHT), Male, Maldives, 11–12 March 2023; pp. 1–6. [CrossRef]
137. Amirpour, S.; Thiringer, T.; Hagstedt, D. Energy Loss Analysis in a SiC/IGBT Propulsion Inverter over Drive Cycles Considering Blanking time MOSFET's Reverse Conduction and the Effect of Thermal Feedback. In Proceedings of the 2020 IEEE Energy Conversion Congress and Exposition (ECCE), Detroit, MI, USA, 11–15 October 2020; pp. 1505–1511.
138. Li, L.; Tang, J.; Zhang, J.Q.; Zhang, J.; Zhu, Y.; Zhang, G.; Liu, P. Overview of Finite-Element Analysis in Simulation of SiC Power Device Packaging. In Proceedings of the 2021 18th China International Forum on Solid State Lighting & 2021 7th International Forum on Wide Bandgap Semiconductors (SSLChina: IFWS), Shenzhen, China, 6–8 December 2021; pp. 53–57. [CrossRef]
139. Li, L.; Ning, P.; Wen, X.; Bian, Y.; Zhang, D. Gate Drive Design for a Hybrid Si IGBT/SiC MOSFET Module. In Proceedings of the 2018 1st Workshop on Wide Bandgap Power Devices and Applications in Asia (WiPDA Asia), Xi'an, China, 16–18 May 2018; pp. 34–41. [CrossRef]
140. Diab, M.S.; Yuan, X. A Quasi-Three-Level PWM Scheme to Combat Motor Overvoltage in SiC-Based Single-Phase Drives. *IEEE Trans. Power Electron.* **2020**, *35*, 12639–12645. [CrossRef]
141. Chen, Z.; Huang, A.Q. High Performance SiC Power Module Based on Repackaging of Discrete SiC Devices. *IEEE Trans. Power Electron.* **2023**, *38*, 9306–9310. [CrossRef]
142. Zhang, Y.; Chen, C.; Liu, T.; Peng, H. A high efficiency dynamic inverter dead-time adjustment method based on an improved GaN HEMTs switching model. *IEEE Trans. Power Electron.* **2022**, *37*, 2667–2683. [CrossRef]
143. Nguyen, H.V.; Dong-Choon, L.; Blaabjerg, F.A. A novel SiC-based multifunctional onboard battery charger for plug-in electric vehicles. *IEEE Trans. Power Electron.* **2021**, *36*, 5635–5646. [CrossRef]
144. Ruffo, R.; Guglielmi, P.; Armando, E. Inverter Side *RL* Filter Precise Design for Motor Overvoltage Mitigation in SiC-Based Drives. *IEEE Trans. Ind. Electron.* **2020**, *67*, 863–873. [CrossRef]
145. DiMarino, C.M.; Mouawad, B.; Johnson, C.M.; Boroyevich, D.; Burgos, R. 10-kV SiC MOSFET Power Module with Reduced Common-Mode Noise and Electric Field. *IEEE Trans. Power Electron.* **2020**, *35*, 6050–6060. [CrossRef]
146. Li, X.; Li, X.; Liu, P.; Guo, S.; Zhang, L.; Huang, A.Q.; Deng, X.; Zhang, B. Achieving Zero Switching Loss in Silicon Carbide MOSFET. *IEEE Trans. Power Electron.* **2019**, *34*, 12193–12199. [CrossRef]

147. Laird, I.; Yuan, X.B.; Scoltock, J.; Forsyth, A.J. A Design Optimization Tool for Maximizing the Power Density of 3-phase DC–AC Converters Using Silicon Carbide (SiC) Devices. *IEEE Trans. Power Electron.* **2018**, *33*, 2913–2932. [CrossRef]
148. Castellazzi, A.; Gurpinar, E.; Wang, Z.; Suliman Hussein, A.; Garcia Fernandez, P. Impact of Wide-Bandgap Technology on Renewable Energy and Smart-Grid Power Conversion Applications Including Storage. *Energies* **2019**, *12*, 4462. [CrossRef]
149. Zaman, H.; Wu, X.; Zheng, X.; Khan, S.; Ali, H. Suppression of Switching Crosstalk and Voltage Oscillations in a SiC MOSFET Based Half-Bridge Converter. *Energies* **2018**, *11*, 3111. [CrossRef]
150. Chen, Z.; Chen, C.; Huang, Q.; Huang, A.Q. Design of High Power Converter with Single Low Ron Discrete SiC Device. In Proceedings of the 2022 IEEE 9th Workshop on Wide Bandgap Power Devices & Applications (WiPDA), Redondo Beach, CA, USA, 7–9 November 2022; pp. 209–214.
151. Kumar, A.; Losito, M.; Moradpour, M.; Gatto, G. Current Source Gate Driver for SiC MOSFETs in Power Electronics Applications. In Proceedings of the 2022 International Symposium on Power Electronics, Electrical Drives, Automation and Motion (SPEEDAM), Sorrento, Italy, 22–24 June 2022; pp. 523–527.
152. Velander, E.; Bohlin, G.; Sandberg, Å.; Wiik, T.; Botling, F.; Lindahl, M.; Zanuso, G.; Nee, H.P. An Ultra Low Loss Inductorless dv/dt Filter Concept for Medium-Power Voltage Source Motor Drive Converters with SiC Devices. *IEEE Trans. Power Electron.* **2018**, *33*, 6072–6081. [CrossRef]
153. He, J.; Li, C.; Jassal, A.; Thiagarajan, N.; Zhang, Y.; Prabhakaran, S.; Feliz, C.; Graham, J.E.; Kang, X. Multi-Domain Design Optimization of dv/dt Filter for SiC-Based Three-Phase Inverters in High-Frequency Motor-Drive Applications. *IEEE Trans. Ind. Appl.* **2019**, *55*, 5214–5222. [CrossRef]
154. Kolar, J.W.; Anderson, J.A.; Mirić, S.; Haider, M.; Guacci, M.; Antivachis, M.; Zulauf, G.; Menzi, D.; Niklaus, P.S.; Miniböck, J.; et al. Application of WBG power devices in future 3-F variable speed drive inverter systems how to handle a double-edged sword. In Proceedings of the 2020 IEEE International Electron Devices Meeting (IEDM), San Francisco, CA, USA, 12–16 December 2020; pp. 27.7.1–27.7.4.
155. Liu, Z.; Li, B.; Lee, F.C.; Li, Q. High-Efficiency High-Density Critical Mode Rectifier/Inverter for WBG-Device-Based On-Board Charger. *IEEE Trans. Ind. Electron.* **2017**, *64*, 9114–9123. [CrossRef]
156. Sun, M.; Zhang, Y.; Gao, X.; Palacios, T. High-Performance GaN Vertical Fin Power Transistors on Bulk GaN Substrates. *IEEE Electron Device Lett.* **2017**, *38*, 509–512. [CrossRef]
157. Hussein, A.; Castellazzi, A. Variable Frequency Control and Filter Design for Optimum Energy Extraction from a SiC Wind Inverter. In Proceedings of the International Power Electronics Conference (IPEC-Niigata 2018–ECCE Asia), Niigata, Japan, 20–24 May 2018.
158. Kogure, H.; Ishikawa, K.; Kohno, Y.; Sakai, T.; Ishigaki, T. Development of low loss inverter system adopted lower harmonic losses technology and ultra compact inverters adopted high power density sic module. In Proceedings of the 2018 20th European Conference on Power Electronics and Applications (EPE'18 ECCE Europe), Riga, Latvia, 17–21 September 2018; pp. P.1–P.7.
159. Torres, R.A.; Dai, H.; Lee, W.; Sarlioglu, B.; Jahns, T. Current-Source Inverter Integrated Motor Drives Using Dual-Gate Four-Quadrant Wide-Bandgap Power Switches. *IEEE Trans. Ind. Appl.* **2021**, *57*, 5183–5198. [CrossRef]
160. Stella, F.; Savio, S.; Vico, E.; Bojoi, R.; Armando, E. Cost Effective 3D Printed Heatsink for Fast Prototyping of WBG Power Converters. In Proceedings of the 2024 IEEE Applied Power Electronics Conference and Exposition (APEC), Long Beach, CA, USA, 25–29 February 2024; pp. 2562–2567. [CrossRef]
161. Osman, A.; Moreno, G.; Myers, S.; Major, J.; Feng, X.; Narumanchi, S.V.; Joshi, Y. Automotive Silicon Carbide Power Module Cooling with a Novel Modular Manifold and Embedded Heat Sink. *J. Electron. Packag.* **2024**, *146*, 021007. [CrossRef]
162. Zachariae, J.; Tiesler, M.; Singh, R.; Benning, T.-A.; Schweikert, C. Silicon Carbide Based Traction Inverter Cooling in Electric Vehicle Using Heat Pipes. *Therm. Sci. Eng. Progress.* **2023**, *46*, 102155. [CrossRef]
163. Torres, R.A.; Dai, H.; Lee, W.; Saviers, K.; Jahns, T.M.; Sarlioglu, B. Investigation of Cooling Techniques and Enclosure Types for Integrated Motor Drives. In Proceedings of the 2022 IEEE Energy Conversion Congress and Exposition (ECCE), Detroit, MI, USA, 9–13 October 2022; pp. 1–8. [CrossRef]
164. Torres, R.A.; Dai, H.; Jahns, T.M.; Sarlioglu, B.; Lee, W. Thermal Analysis of Housing-Cooled Integrated Motor Drives. In Proceedings of the 2021 IEEE Transportation Electrification Conference & Expo (ITEC), Chicago, IL, USA, 21–25 June 2021; pp. 1–6. [CrossRef]
165. Mademlis, G.; Orbay, R.; Liu, Y.; Sharma, N.; Arvidsson, R.; Thiringer, T. Multidisciplinary Cooling Design Tool for Electric Vehicle SiC Inverters Utilizing Transient 3D-CFD Computations. *eTransportation* **2021**, *7*, 100092. [CrossRef]
166. Abramushkina, E.; Zhaksylyk, A.; Geury, T.; El Baghdadi, M.; Hegazy, O. A Thorough Review of Cooling Concepts and Thermal Management Techniques for Automotive WBG Inverters: Topology, Technology and Integration Level. *Energies* **2021**, *14*, 4981. [CrossRef]
167. Zeng, Z.; Zhang, X.; Blaabjerg, F.; Chen, H.; Sun, T. Stepwise Design Methodology and Heterogeneous Integration Routine of Air-Cooled SiC Inverter for Electric Vehicle. *IEEE Trans. Power Electron.* **2020**, *35*, 3973–3988. [CrossRef]

168. Alizadeh, M.; Rodriguez, R.; Bauman, J.; Emadi, A. Optimal Design of Integrated Heat Pipe Air-cooled System Using TLBO algorithm for SiC MOSFET Converters. *IEEE Open J. Power Electron.* **2020**, *1*, 103–112. [CrossRef]
169. Wu, T.; Wang, Z.; Ozpineci, B.; Chinthavali, M.; Campbell, S. Automated Heatsink Optimization for Air-cooled Power Semiconductor Modules. *IEEE Trans. Power Electron.* **2019**, *34*, 5027–5031. [CrossRef]
170. Michalak, A.; Zaman, M.S.; Tayyara, O.; Nasr, M.; Da Silva, C.; Mills, J.K.; Trescases, O.; Amon, C.H. A Thermal Management Design Methodology for Advanced Power Electronics Utilizing Genetic Optimization and Additive Manufacturing Techniques. In Proceedings of the 2020 19th IEEE Intersociety Conference on Thermal and Thermomechanical Phenomena in Electronic Systems (ITherm), Orlando, FL, USA, 21–23 July 2020; pp. 547–557.
171. Gurpinar, E.; Sahu, R.; Ozpineci, B. Heat Sink Design for WBG Power Modules Based on Fourier Series and Evolutionary Multi-Objective Multi-Physics Optimization. *IEEE Open J. Power Electron.* **2021**, *2*, 559–569. [CrossRef]
172. Yao, R.; Zhu, Z.; Li, H.; Lai, W.; Chen, X.; Iannuzzo, F.; Liu, R.; Luo, X. A Double-Sided Cooling Approach of Discrete SiC MOSFET Device Based on Press-Pack Package. *IEEE Open J. Power Electron.* **2024**, *5*, 1629–1640. [CrossRef]
173. Chen, R.; Wang, F.F. SiC and GaN Devices with Cryogenic Cooling. *IEEE Open J. Power Electron.* **2021**, *2*, 315–326. [CrossRef]
174. Pahinkar, D.G.; Boteler, L.; Ibitayo, D.; Narumanchi, S.; Paret, P.; DeVoto, D.; Major, J.; Graham, S. Liquid-cooled Aluminum Silicon Carbide Heat Sinks for Reliable Power Electronics Packages. *J. Electron. Packag.* **2019**, *141*, 041001. [CrossRef]
175. Tang, G.; Wai, L.C.; Boon Lim, S.; Lau, B.L.; Kazunori, Y.; Zhang, X.W. Thermal Analysis, Characterization and Material Selection for SiC Device Based Intelligent Power Module (IPM). In Proceedings of the 2020 IEEE 70th Electronic Components and Technology Conference (ECTC), Orlando, FL, USA, 3–30 June 2020; pp. 2078–2085.
176. Mademlis, G.; Orbay, R.; Liu, Y.; Sharma, N. Designing Thermally Uniform Heatsink with Rectangular Pins for High-Power Automotive SiC Inverters. In Proceedings of the IECON 2020 The 46th Annual Conference of the IEEE Industrial Electronics Society, Singapore, 18–21 October 2020; pp. 1317–1322.
177. Becker, N.; Bulovic, S.; Bittner, R.; Herzer, R. Thermal Simulation for Power Density Optimization of SiC-MOSFET Automotive Inverter. In Proceedings of the CIPS 2020 11th International Conference on Integrated Power Electronics Systems, Berlin, Germany, 24–26 March 2020; pp. 1–6.
178. Catalano, A.P.; Scognamillo, C.; Castellazzi, A.; d'Alessandro, V. Optimum Thermal Design of High-Voltage Double-Sided Cooled Multi-Chip SiC Power Modules. In Proceedings of the 2019 25th International Workshop on Thermal Investigations of ICs and Systems (THERMINIC), Lecco, Italy, 25–27 September 2019; pp. 1–4.
179. McPherson, B.; McGee, B.; Simco, D.; Olejniczak, K.; Passmore, B. Direct Liquid Cooling of High Performance Silicon Carbide (SiC) Power Modules. In Proceedings of the 2017 IEEE Int. Workshop on Integrated Power Packaging (IWIPP), Delft, The Netherlands, 5–7 April 2017; pp. 1–5.
180. Acharya, S.; Anurag, A.; Bhattacharya, S.; Pellicone, D. Performance Evaluation of a Loop Thermosyphon-Based Heatsink for High-Power SiC-Based Converter Applications. *IEEE Trans. Compon. Packag. Manuf. Technol.* **2020**, *10*, 99–110. [CrossRef]
181. Lee, W.; Torres, R.A.; Dai, H.; Jahns, T.M.; Sarlioglu, B. Integration and Cooling Strategies for WBG-based Current-Source Inverters-Based Motor Drives. In Proceedings of the 2021 IEEE Energy Conversion Congress and Exposition (ECCE), Vancouver, BC, Canada, 10–14 October 2021; pp. 5225–5232. [CrossRef]
182. Han, S.-G.; Lee, W.-H.; Hwang, D.-Y.; Park, S.-M.; Choi, J.-H.; Joo, D.-M. Thermal Design and Development of a Inverter Considering the Switch Characteristics of Wide Band Gap Power semiconductor. In Proceedings of the 2021 24th International Conference on Electrical Machines and Systems (ICEMS), Gyeongju, Republic of Korea, 31 October–3 November 2021; pp. 2138–2144. [CrossRef]
183. Emon, A.I.; Mustafeez-ul-Hassan; Mirza, A.B.; Kaplun, J.; Vala, S.S.; Luo, F. A Review of High-Speed GaN Power Modules: State of the Art, Challenges, and Solutions. *IEEE J. Emerg. Sel. Top. Power Electron.* **2023**, *11*, 2707–2729. [CrossRef]
184. Singh, S.; Chaudhary, T.; Khanna, G. Recent Advancements in Wide Band Semiconductors (SiC and GaN) Technology for Future Devices. *Silicon* **2022**, *14*, 5793–5800. [CrossRef]
185. Kumar, A.; Moradpour, M.; Losito, M.; Franke, W.-T.; Ramasamy, S.; Baccoli, R.; Gatto, G. Wide Band Gap Devices and Their Application in Power Electronics. *Energies* **2022**, *15*, 9172. [CrossRef]
186. Rafin, S.M.S.H.; Ahmed, R.; Mohammed, O.A. Wide Band Gap Semiconductor Devices for Power Electronic Converters. In Proceedings of the 2023 Fourth International Symposium on 3D Power Electronics Integration and Manufacturing (3D-PEIM), Miami, FL, USA, 1–3 February 2023; pp. 1–8. [CrossRef]
187. Bérubé, Y.; Ghazanfari, A.; Blanchette, H.F.; Perreault, C.; Zaghib, K. Recent Advances in Wide Bandgap Devices for Automotive Industry. In Proceedings of the IECON 2020 The 46th Annual Conference of the IEEE Industrial Electronics Society, Singapore, 18–21 October 2020; pp. 2557–2564. [CrossRef]
188. Setera, B.; Christou, A. Challenges of Overcoming Defects in Wide Bandgap Semiconductor Power Electronics. *Electronics* **2022**, *11*, 10. [CrossRef]
189. Wang, Y.; Ding, Y.; Yin, Y. Reliability of Wide Band Gap Power Electronic Semiconductor and Packaging: A Review. *Energies* **2022**, *15*, 6670. [CrossRef]

190. Iannaccone, G.; Sbrana, C.; Morelli, I.; Strangio, S. Power Electronics Based on Wide-Bandgap Semiconductors: Opportunities and Challenges. *IEEE Access* **2021**, *9*, 139446–139456. [CrossRef]
191. Lee, H.; Smet, V.; Tummala, R. A Review of SiC Power Module Packaging Technologies: Challenges, Advances, and Emerging Issues. *IEEE J. Emerg. Sel. Top. Power Electron.* **2020**, *8*, 239–255. [CrossRef]
192. Chen, J.; Du, X.; Luo, Q.; Zhang, X.; Sun, P.; Zhou, L. A Review of Switching Oscillations of Wide Bandgap Semiconductor Devices. *IEEE Trans. Power Electron.* **2020**, *35*, 13182–13199. [CrossRef]
193. Bader, S.J.; Lee, H.; Chaudhuri, R.; Huang, S.; Hickman, A.; Molnar, A.; Xing, H.G.; Jena, D.; Then, H.W.; Chowdhury, N.; et al. Prospects for Wide Bandgap and Ultrawide Bandgap CMOS Devices. *IEEE Trans. Electron Devices* **2020**, *67*, 4010–4020. [CrossRef]
194. Ferreira, J.A.; Wilson, P. Impact ITRW: How Can WBG Power Semicond. Break Through? *IEEE Open J. Power Electron.* **2021**, *2*, 327–335. [CrossRef]
195. Kizilyalli, I.C.; Xu, Y.A.; Carlson, E.; Manser, J.; Cunningham, D.W. Current and future directions in power electronic devices and circuits based on wide band-gap semiconductors. In Proceedings of the 2017 IEEE 5th Workshop on Wide Bandgap Power Devices and Applications (WiPDA), Albuquerque, NM, USA, 30 October–1 November 2017; p. 417. [CrossRef]
196. Yuan, X.; Laird, I.; Walder, S. Opportunities, Challenges, and Potential Solutions in the Application of Fast-Switching SiC Power Devices and Converters. *IEEE Trans. Power Electron.* **2021**, *36*, 3925–3945. [CrossRef]
197. Matallana, A.; Ibarra, E.; López, I.; Andreu, J.; Garate, J.I.; Jordà, X.; Rebollo, J. Power Module Electronics in HEV/EV Applications: New Trends in Wide-Bandgap Semiconductor Technologies and Design Aspects. *Renew. Sustain. Energy Rev.* **2019**, *113*, 109264. [CrossRef]
198. Qi, F.; Wang, M.; Xu, L. Investigation and Review of Challenges in a High-Temperature 30-KVA Three-Phase Inverter Using SiC MOSFETs. *IEEE Trans. Ind. Appl.* **2018**, *54*, 2483–2491. [CrossRef]
199. Kizilyalli, I.C.; Carlson, E.P.; Cunningham, D.W. Barriers to the Adoption of Wide-Bandgap Semiconductors for Power Electronics. In Proceedings of the 2018 IEEE International Electron Devices Meeting (IEDM), San Francisco, CA, USA, 1–5 December 2018; pp. 19.6.1–19.6.4. [CrossRef]
200. Yuan, X. Application of silicon carbide (SiC) power devices: Opportunities, challenges and potential solutions. In Proceedings of the IECON 2017-43rd Annual Conference of the IEEE Industrial Electronics Society, Beijing, China, 29 October–1 November 2017; pp. 893–900. [CrossRef]
201. Zhang, Z.; Hu, Y.; Chen, X.; Jewell, G.W.; Li, H. A Review on Conductive Common-Mode EMI Suppression Methods in Inverter Fed Motor Drives. *IEEE Access* **2021**, *9*, 18345–18360. [CrossRef]
202. Weiss, P.; Bauer, C.; Jung, R.; Berberich, K. Double Side Cooled Modules Enable Future Generation of SiC-Traction-Inverters, PCIM Europe digital days 2021. In Proceedings of the International Exhibition and Conference for Power Electronics, Intelligent Motion, Renewable Energy and Energy Management, Online, 3–7 May 2021; pp. 1–6.
203. Jones, E.A.; Wang, F.F.; Costinett, D. Review of commercial GaN power devices and GaN-based converter design challenges. *IEEE J. Emerg. Sel. Top. Power Electron.* **2016**, *4*, 707–719. [CrossRef]
204. Available online: https://us.metoree.com/categories/sic-mosfet/ (accessed on 15 December 2024).
205. Blaschke, F. The principle of field-orientation as applied to the new transvector closed-loop system for rotating-field machines. *Siemens Rev.* **1972**, *34*, 217–220.
206. Carbone, L.; Cosso, S.; Kumar, K.; Marchesoni, M.; Passalacqua, M.; Vaccaro, L. Induction Motor Field-Oriented Sensorless Control with Filter and Long Cable. *Energies* **2022**, *15*, 1484. [CrossRef]
207. Domínguez, J.R.; Dueñas, I.; Ortega-Cisneros, S. Discrete-Time Modeling and Control Based on Field Orientation for Induction Motors. *IEEE Trans. Power Electron.* **2020**, *35*, 8779–8793. [CrossRef]
208. Akhtar, M.J.; Behera, R.K. Space Vector Modulation for Distributed Inverter-Fed Induction Motor Drive for Electric Vehicle Application. *IEEE J. Emerg. Sel. Top. Power Electron.* **2021**, *9*, 379–389. [CrossRef]
209. Jo, G.-J.; Choi, J.-W. Gopinath Model-Based Voltage Model Flux Observer Design for Field-Oriented Control of Induction Motor. *IEEE Trans. Power Electron.* **2019**, *34*, 4581–4592. [CrossRef]
210. Mehedi, I.M.; Saad, N.; Magzoub, M.A.; Al-Saggaf, U.M.; Milyani, A.H. Simulation Analysis and Experimental Evaluation of Improved Field-Oriented Controlled Induction Motors Incorporating Intelligent Controllers. *IEEE Access* **2022**, *10*, 18380–18394. [CrossRef]
211. Cheerangal, M.J.; Jain, A.K.; Das, A. Multiple Fault Tolerant Control Strategy for Rotor Field Oriented Induction Motor Drive Fed from CHB Converter with Redundant Cells. *IEEE Trans. Power Electron.* **2023**, *38*, 852–861. [CrossRef]
212. Abbasi, H.; Ghanbari, M.; Ebrahimi, R.; Jannati, M. IRFOC of Induction Motor Drives Under Open-Phase Fault Using Balanced and Unbalanced Transformation Matrices. *IEEE Trans. Ind. Electron.* **2021**, *68*, 9160–9173. [CrossRef]
213. Devanshu, A.; Singh, M.; Kumar, N. An Improved Nonlinear Flux Observer Based Sensorless FOC IM Drive with Adaptive Predictive Current Control. *IEEE Trans. Power Electron.* **2020**, *35*, 652–666. [CrossRef]
214. Shabandokht-Zarami, M.; Ghanbari, M.; Alibeiki, E.; Jannati, M. A Modified FOC Strategy with Optimal Rotor Flux for FTC of Star-Connected TPIMDs Against Single-Phase Open Fault. *IEEE Can. J. Electr. Comput. Eng.* **2021**, *44*, 83–93. [CrossRef]

215. Prieto, I.G.; Duran, M.J.; Garcia-Entrambasaguas, P.; Bermudez, M. Field-Oriented Control of Multiphase Drives with Passive Fault Tolerance. *IEEE Trans. Ind. Electron.* **2020**, *67*, 7228–7238. [CrossRef]
216. Available online: https://www.st.com/en/applications/industrial-motor-control/3-phase-field-oriented-control-foc (accessed on 15 December 2024).
217. Białoń, T.; Niestrój, R.; Michalak, J.; Pasko, M. Induction Motor PI Observer with Reduced-Order Integrating Unit. *Energies* **2021**, *14*, 4906. [CrossRef]
218. Wang, F.; Zhang, Z.; Mei, X.; Rodríguez, J.; Kennel, R. Advanced Control Strategies of Induction Machine: Field Oriented Control, Direct Torque Control and Model Predictive Control. *Energies* **2018**, *11*, 120. [CrossRef]
219. Fnaiech, M.A.; Guzinski, J.; Trabelsi, M.; Kouzou, A.; Benbouzid, M.; Luksza, K. MRAS-Based Switching Linear Feedback Strategy for Sensorless Speed Control of Induction Motor Drives. *Energies* **2021**, *14*, 3083. [CrossRef]
220. Pal, A.; Das, S.; Chattopadhyay, A. An improved rotor flux space vector based MRAS for field-oriented control of induction motor drives. *IEEE Trans. Power Electron.* **2018**, *33*, 5131–5141. [CrossRef]
221. Dehghan-Azad, E.; Gadoue, S.; Atkinson, D.; Slater, H.; Barrass, P.; Blaabjerg, F. Sensorless control of im based on stator-voltage mras for limp-home ev applications. *IEEE Trans. Power Electron.* **2018**, *33*, 1911–1921. [CrossRef]
222. Khadar, S.; Abu-Rub, H.; Kouzou, A. Sensorless Field-Oriented Control for Open-End Winding Five-Phase Induction Motor with Parameters Estimation. *IEEE Open J. Ind. Electron. Soc.* **2021**, *2*, 266–279. [CrossRef]
223. Hamdi, E.; Ramzi, T.; Atif, I.; Mohamed, M.F. Real time implementation of indirect rotor flux oriented control of a five-phase induction motor with novel rotor resistance adaption using sliding mode observer. *J. Frankl. Inst.* **2018**, *355*, 2112–2141.
224. Prabhakar, K.K.; Reddy, C.U.; Kumar, P.; Singh, A.K. A New Reference Flux Linkage Selection Technique for Efficiency Improvement of Direct Torque Controlled IM Drive. *IEEE J. Emerg. Sel. Top. Power Electron.* **2020**, *8*, 3751–3762. [CrossRef]
225. Savarapu, S.; Qutubuddin, M.; Narri, Y. Modified Brain Emotional Controller-Based Ripple Minimization for SVM-DTC of Sensorless Induction Motor Drive. *IEEE Access* **2022**, *10*, 40872–40887. [CrossRef]
226. Alsofyani, I.M.; Bak, Y.; Lee, K.-B. Fast Torque Control and Minimized Sector-Flux Droop for Constant Frequency Torque Controller Based DTC of Induction Machines. *IEEE Trans. Power Electron.* **2019**, *34*, 12141–12153. [CrossRef]
227. Alsofyani, I.M.; Idris, N.R.N.; Lee, K.-B. Dynamic Hysteresis Torque Band for Improving the Performance of Lookup-Table-Based DTC of Induction Machines. *IEEE Trans. Power Electron.* **2018**, *33*, 7959–7970. [CrossRef]
228. Holakooie, M.H.; Ojaghi, M.; Taheri, A. Direct Torque Control of Six-Phase Induction Motor with a Novel MRAS-Based Stator Resistance Estimator. *IEEE Trans. Ind. Electron.* **2018**, *65*, 7685–7696. [CrossRef]
229. Kumar, R.H.; Iqbal, A.; Lenin, N.C. Review of recent advancements of direct torque control in induction motor drives–a decade of progress. *IET Power Electron.* **2018**, *11*, 1–15. [CrossRef]
230. El Ouanjli, N.; Derouich, A.; El Ghzizal, A.; Motahhir, S.; Chebabhi, A.; El Mourabit, Y.; Taoussi, M. Modern improvement techniques of direct torque control for induction motor drives-a review. *Prot. Control Mod. Power Syst.* **2019**, *4*, 1–12. [CrossRef]
231. Peter, A.K.; Mathew, J.; Gopakumar, K. A simplified DTC-SVPWM scheme for induction motor drives using a single PI controller. *IEEE Trans. Power Electron.* **2023**, *38*, 750–761. [CrossRef]
232. Benevieri, A.; Maragliano, G.; Marchesoni, M.; Passalacqua, M.; Vaccaro, L. Induction Motor Direct Torque Control with Synchronous PWM. *Energies* **2021**, *14*, 5025. [CrossRef]
233. Naganathan, P.; Srinivas, S. MTPA Associated DTC Methodologies for Enhanced Performance and Energy Savings in Electric Vehicle Mobility with Induction Motor Drive. *IEEE Trans. Transp. Electrif.* **2022**, *8*, 1853–1862. [CrossRef]
234. Pimkumwong, N.; Wang, M.S. Full-order observer for direct torque control of induction motor based on constant V/F control technique. *ISA Trans.* **2018**, *73*, 189–200. [CrossRef]
235. Ammar, A.; Bourek, A.; Benakcha, A. Robust SVM-direct torque control of induction motor based on sliding mode controller and sliding mode observer. *Front. Energy* **2020**, *14*, 836–849. [CrossRef]
236. Hamdi, E.; Ramzi, T.; Atif, I.; Mohamed, M.F. Adaptive direct torque control using Luenberger-sliding mode observer for online stator resistance estimation for five-phase induction motor drives. *Elect. Eng.* **2018**, *100*, 1639–1649.
237. Abdelkarim, A.; Aissa, K.; Brahim, M.; Tarek, A.; Younes, A. Feedback linearization based sensorless direct torque control using stator flux MRAS-sliding mode observer for induction motor drive. *ISA Trans.* **2020**, *98*, 382–392.
238. Chagam, V.S.R.; Devabhaktuni, S. Enhanced Low-Speed Characteristics with Constant Switching Torque-Controller-Based DTC Technique of Five-Phase Induction Motor Drive with FOPI Control. *IEEE Trans. Ind. Electron.* **2023**, *70*, 10789–10799. [CrossRef]
239. Wu, X.; Huang, W.; Lin, X.; Jiang, W.; Zhao, Y.; Zhu, S. Direct Torque Control for Induction Motors Based on Minimum Voltage Vector Error. *IEEE Trans. Ind. Electron.* **2021**, *68*, 3794–3804. [CrossRef]
240. Tiitinen, P.; Surandra, M. The next generation motor control method, DTC direct torque control. In Proceedings of the International Conference on Power Electronics, Drives and Energy Systems for Industrial Growth, New Delhi, India, 8–11 January 1996; Volume 1, pp. 37–43.
241. Çavuş, B.; Aktaş, M. MPC-Based Flux Weakening Control for Induction Motor Drive with DTC for Electric Vehicles. *IEEE Trans. Power Electron.* **2023**, *38*, 4430–4439. [CrossRef]

242. Rodriguez, J.; Garcia, C.; Mora, A.; Flores-Bahamonde, F.; Acuna, P.; Novak, M.; Zhang, Y.; Tarisciotti, L.; Davari, S.A.; Zhang, Z.; et al. Latest Advances of Model Predictive Control in Electrical Drives—Part I: Basic Concepts and Advanced Strategies. *IEEE Trans. Power Electron.* **2022**, *37*, 3927–3942. [CrossRef]
243. Arshad, M.H.; Abido, M.A.; Salem, A.; Elsayed, A.H. Weighting Factors Optimization of Model Predictive Torque Control of Induction Motor Using NSGA-II with TOPSIS Decision Making. *IEEE Access* **2019**, *7*, 177595–177606. [CrossRef]
244. Aziz, A.G.M.A.; Rez, H.; Diab, A.A.Z. Robust Sensorless Model-Predictive Torque Flux Control for High-Performance Induction Motor Drives. *Mathematics* **2021**, *9*, 403. [CrossRef]
245. Gonzalez-Prieto, I.; Duran, M.; Aciego, J.; Martin, C.; Barrero, F. Model predictive control of six-phase induction motor drives using virtual voltage vectors. *IEEE Trans. Ind. Electron.* **2018**, *65*, 27–37. [CrossRef]
246. Zhou, Y.; Chen, G. Predictive DTC Strategy with Fault-Tolerant Function for Six-Phase and Three-Phase PMSM Series-Connected Drive System. *IEEE Trans. Ind. Electron.* **2018**, *65*, 9101–9112. [CrossRef]
247. Chebaani, M.; Ebeed, M.; Abdellatif, W.S.E.; Elbarbary, Z.M.S.; Nouraldin, N.A. Design and Implementation of an Improved Finite-State Predictive Direct Torque Control for Induction Motor with New Weighting Factor Elimination. *IEEE Access* **2023**, *11*, 58169–58187. [CrossRef]
248. Yang, A.; Lu, Z. Multiscalar Model-Based Predictive Torque Control Without Weighting Factors and Current Sensors for Induction Motor Drives. *IEEE J. Emerg. Sel. Top. Power Electron.* **2022**, *10*, 5785–5797. [CrossRef]
249. Wang, T.; Wang, Y.; Zhang, Z.; Li, Z.; Hu, C.; Wang, F. Comparison and analysis of predictive control of induction motor without weighting factors. *Energy Rep.* **2023**, *9*, 558–568. [CrossRef]
250. Wróbel, K.; Serkies, P.; Szabat, K. Model Predictive Base Direct Speed Control of Induction Motor Drive—Continuous and Finite Set Approaches. *Energies* **2020**, *13*, 1193. [CrossRef]
251. Novak, M.; Xie, H.T.; Dragicevic, T.; Wang, F.X.; Rodríguez, J.; Blaabjerg, F. Optimal Cost Function Parameter Design in Predictive Torque Control (PTC) Using Artificial Neural Networks (ANN). *IEEE Trans. Ind. Electron.* **2021**, *68*, 7309–7319. [CrossRef]
252. Muddineni, V.P.; Bonala, A.K.; Sandepudi, S.R. Grey Relational Analysis-Based Objective Function Optimization for Predictive Torque Control of Induction Machine. *IEEE Trans. Ind. Appl.* **2021**, *57*, 835–844. [CrossRef]
253. Zhang, Y.; Yin, Z.; Li, W.; Liu, J.; Zhang, Y. Adaptive Sliding-Mode-Based Speed Control in Finite Control Set Model Predictive Torque Control for Induction Motors. *IEEE Trans. Power Electron.* **2021**, *36*, 8076–8087. [CrossRef]
254. Norambuena, M.; Rodríguez, J.; Zhang, Z.B.; Wang, F.X.; Garcia, C.; Kennel, R. A Very Simple Strategy for High-Quality Performance of AC Machines Using Model Predictive Control. *IEEE Trans. Power Electron.* **2019**, *34*, 794–800. [CrossRef]
255. Mamdouh, M.; Abido, M.A. Efficient Predictive Torque Control for Induction Motor Drive. *IEEE Trans. Ind. Electron.* **2019**, *66*, 6757–6767. [CrossRef]
256. Geyer, T. Algebraic tuning guidelines for model predictive torque and flux control. *IEEE Trans. Ind. Appl.* **2018**, *51*, 4464–4475. [CrossRef]
257. Azab, M. Comparative Study of BLDC Motor Drive with Different Approaches: FCS-Model Predictive Control and Hysteresis Current Control. *World Electric. Vehicle. J.* **2022**, *13*, 112. [CrossRef]
258. Wang, X.; Zhang, H.; Sun, S.; Gao, Y.; Jin, B. Energy Recovery and Utilization Efficiency Improvement for Motor-Driven System Using Dynamic Energy Distribution Method. *IEEE Trans. Veh. Technol.* **2022**, *71*, 10327–10336. [CrossRef]
259. Zhang, Y.; Yuan, W.; Fu, R.; Wang, C. Design of an Energy-Saving Driving Strategy for Electric Buses. *IEEE Access* **2019**, *7*, 157693–157706. [CrossRef]
260. Zhang, Y.; Zhang, Y.; Ai, Z.; Murphey, Y.L.; Zhang, J. Energy Optimal Control of Motor Drive System for Extending Ranges of Electric Vehicles. *IEEE Trans. Ind. Electron.* **2021**, *68*, 1728–1738. [CrossRef]
261. Wang, S.; Zhang, Q.; Kang, G.; Fan, X.; Zhang, S.; Bao, J. An Optimization Method for Improving Efficiency of Electric Propulsion System of Electric Seaplane. *IEEE Access* **2023**, *11*, 31052–31061. [CrossRef]
262. Almani, M.N.; Hussain, G.A.; Zaher, A.A. An Improved Technique for Energy-Efficient Starting and Operating Control of Single Phase Induction Motors. *IEEE Access* **2021**, *9*, 12446–12462. [CrossRef]
263. Babu, V.R.; Maity, T.; Ramesh, G. Speed Control and Optimum Efficiency of Induction Motor Driven Ventilation Fan in Mines. In Proceedings of the 2019 IEEE International Conference on Electrical, Computer and Communication Technologies (ICECCT), Coimbatore, India, 20–22 February 2019; pp. 1–4. [CrossRef]
264. Golsorkhi, M.S.; Binandeh, H.; Savaghebi, M. Online Efficiency Optimization and Speed Sensorless Control of Single-Phase Induction Motors. *Appl. Sci.* **2021**, *11*, 8863. [CrossRef]
265. Nassiri, S.; Labbadi, M.; Chatri, C.; Cherkaoui, M. Optimal Efficiency Controller Design of Pumping Systems. In Proceedings of the 2024 American Control Conference (ACC), Toronto, ON, Canada, 8–12 July 2024; pp. 4493–4498. [CrossRef]
266. Shukla, N.K.; Srivastava, R.; Mirjalili, S. A hybrid dragonfly algorithm for efficiency optimization of induction motors. *Sensors* **2022**, *22*, 2594. [CrossRef]
267. Ma, Z.; Sun, D. Energy Recovery Strategy Based on Ideal Braking Force Distribution for Regenerative Braking System of a Four-Wheel Drive Electric Vehicle. *IEEE Access* **2020**, *8*, 136234–136242. [CrossRef]

268. Xu, Q.; Wang, F.; Zhang, X.; Cui, S. Research on the Efficiency Optimization Control of the Regenerative Braking System of Hybrid Electrical Vehicle Based on Electrical Variable Transmission. *IEEE Access* **2019**, *7*, 116823–116834. [CrossRef]
269. Dabral, S.; Basak, S.; Chakraborty, C. Regenerative Braking Efficiency Enhancement Using Pole-Changing Induction Motor. *IEEE Trans. Transp. Electrif.* **2024**, *10*, 7580–7590. [CrossRef]
270. Ahamad, N.B.B.; Su, C.-L.; Zhaoxia, X.; Vasquez, J.C.; Guerrero, J.M.; Liao, C.-H. Energy Harvesting from Harbor Cranes with Flywheel Energy Storage Systems. *IEEE Trans. Ind. Appl.* **2019**, *55*, 3354–3364. [CrossRef]
271. Becker, M.; Stender, M.; Wallscheid, O. Nonlinear Efficiency-Optimal Model Predictive Torque Control of Induction Machines. *IEEE J. Emerg. Sel. Top. Power Electron.* **2024**, *12*, 4740–4753. [CrossRef]
272. Available online: https://new.abb.com/drives/dtc (accessed on 15 December 2024).
273. Available online: https://www.danfoss.com/en/about-danfoss/our-businesses/drives/ (accessed on 15 December 2024).
274. Available online: https://www.deltaww.com/en-US/products/AC-Motor-Drives/ALL/ (accessed on 15 December 2024).
275. Available online: https://www.eaton.com/us/en-us/products/controls-drives-automation-sensors/variable-frequency-drives.html (accessed on 15 December 2024).
276. Available online: https://www.emotron.com/products/variable-frequency-drives-vdf/ (accessed on 15 December 2024).
277. Available online: https://www.fujielectric.com/products/drives_inverters/ac_drives_lv/index.html (accessed on 15 December 2024).
278. Available online: https://hitachiacdrive.com/ (accessed on 15 December 2024).
279. Available online: https://www.inomaxtechnology.com/product-category/motion-control/variable-frequency-drives/ (accessed on 15 December 2024).
280. Available online: https://www.invertekdrives.com/ (accessed on 15 December 2024).
281. Available online: https://emea.mitsubishielectric.com/fa/products/drv/inv (accessed on 15 December 2024).
282. Available online: https://acim.nidec.com/en/drives/control-techniques/Products (accessed on 15 December 2024).
283. Available online: https://industrial.omron.eu/en/products/variable-speed-drives (accessed on 15 December 2024).
284. Available online: https://www.rockwellautomation.com/en-gb/products/hardware/allen-bradley/vfd.html (accessed on 15 December 2024).
285. Available online: https://www.se.com/us/en/product-category/2900-variable-speed-drives/ (accessed on 15 December 2024).
286. Available online: https://www.siemens.com/us/en/products/drives/sinamics-electric-drives.html (accessed on 15 December 2024).
287. Available online: https://www.toshiba.com/tic/motors-drives (accessed on 15 December 2024).
288. Available online: https://www.weg.net/catalog/weg/US/en/Drives/Variable-Speed-Drives/c/GLOBAL_WDC_DRV_IF (accessed on 15 December 2024).
289. Available online: https://www.yaskawa.com/products/drives/industrial-ac-drives (accessed on 15 December 2024).
290. Available online: https://literature.rockwellautomation.com/idc/groups/literature/documents/td/750-td100_-en-p.pdf (accessed on 15 December 2024).
291. Available online: https://literature.rockwellautomation.com/idc/groups/literature/documents/wp/drives-wp002_-en-p.pdf (accessed on 15 December 2024).

Disclaimer/Publisher's Note: The statements, opinions and data contained in all publications are solely those of the individual author(s) and contributor(s) and not of MDPI and/or the editor(s). MDPI and/or the editor(s) disclaim responsibility for any injury to people or property resulting from any ideas, methods, instructions or products referred to in the content.